Annu. Rev. Biochem. 2005. 74:129–77
doi: 10.1146/annurev.biochem.74.061903.155440

First published online as a Review in Advance on February 25, 2005

STRUCTURAL INSIGHTS INTO TRANSLATIONAL FIDELITY

James M. Ogle and V. Ramakrishnan
Medical Research Council Laboratory of Molecular Biology, Cambridge CB2 2QH, United Kingdom; email: james.ogle@cantab.net, ramak@mrc-lmb.cam.ac.uk

Key Words ribosome, crystallography, decoding, accuracy, antibiotics

■ **Abstract** The underlying basis for the accuracy of protein synthesis has been the subject of over four decades of investigation. Recent biochemical and structural data make it possible to understand at least in outline the structural basis for tRNA selection, in which codon recognition by cognate tRNA results in the hydrolysis of GTP by EF-Tu over 75 Å away. The ribosome recognizes the geometry of codon-anticodon base pairing at the first two positions but monitors the third, or wobble position, less stringently. Part of the additional binding energy of cognate tRNA is used to induce conformational changes in the ribosome that stabilize a transition state for GTP hydrolysis by EF-Tu and subsequently result in accelerated accommodation of tRNA into the peptidyl transferase center. The transition state for GTP hydrolysis is characterized, among other things, by a distorted tRNA. This picture explains a large body of data on the effect of antibiotics and mutations on translational fidelity. However, many fundamental questions remain, such as the mechanism of activation of GTP hydrolysis by EF-Tu, and the relationship between decoding and frameshifting.

CONTENTS

THE ACCURACY OF GENE EXPRESSION

Throughout biology, genomes are maintained and expressed with remarkable fidelity. However, the overall accuracy of gene expression is not as high as is theoretically possible. The accuracy of each process involved represents a compromise that optimizes the evolutionary fitness of the organism. Thus, replication of the genome, which transmits genetic information from one generation to the next, is extremely accurate, with error rates as low as 10^{-8} in bacteria or below 10^{-10} in eukaryotes (1). Not surprisingly, DNA replication has sophisticated error correction mechanisms, including editing and repair. The error rate of transcription in vivo in *Escherichia coli* has been estimated to be 1.4×10^{-4} per nucleotide and thus around 4×10^{-4} per codon (2, 3), and in any case, it is considerably lower than that of replication.

Error rates of translation in vivo have been estimated to be on the order of 10^{-3}–10^{-4} (4). Errors in translation can arise from incorrect aminoacylation of a particular tRNA by synthetases, selection of the incorrect tRNA by the ribosome, or frameshifting during translation. The tRNA aminoacylation step has been shown to be very accurate, owing to enzymatic selectivity mechanisms precisely adapted to the most closely related amino acids for each aminoacyl-tRNA synthetase (5). For example, because of a "double sieve" editing mechanism (6–8), Ile-$tRNA^{Ile}$-synthetase can exclude Val with an efficiency of 1:40,000, i.e., 2.5×10^{-5} (9, 10). Therefore, an overall implication of the in vivo error rate values is that decoding, or codon-dependent selection of aminoacyl tRNA by the ribosome, may be the limiting factor in the accuracy of gene expression or at least makes a somewhat larger contribution to error rates compared to tRNA aminoacylation. However, for certain hyperaccurate ribosomal mutants, the fidelity of transcription might limit the overall accuracy (11). Indeed, it is perhaps reasonable to assume that there is no evolutionary need for the ribosome to be significantly more accurate than the limit imposed on overall gene expression by transcription, if other advantages (such as a higher speed of protein synthesis) can be gained for a certain trade-off

in translational accuracy. In this review, we discuss how recent structures of the ribosome have shed light on its role in translational accuracy and clarified many long-standing issues.

SPECIFICITY OF BASE PAIRING

The role of the specificity of base pairing in the replication and expression of genetic information has often been misunderstood. Shortly after their discovery of the double-helical structure of DNA, Watson & Crick (12) proposed that the same forces that direct the formation of a double helix in solution are also responsible for the maintenance and expression of genetic information in biology. Thus, the high specificity of these processes was proposed to be a direct result of the specificity of the hydrogen bonds formed in base pairing, a view that permeates many textbooks to this day. This idea was extended to translation by Crick, who in his famous adaptor hypothesis proposed that a small nucleic acid adaptor, now known to be tRNA, would base pair with the genetic template and bring along a covalently attached amino acid (13). In an early view, Crick and his colleagues believed that base-pairing interactions alone would account for the specificity of decoding:

> Now imagine that such an amino acid-trinucleotide were to diffuse into an incorrect place on the template, such that *two* of its bases were hydrogen-bonded, though not the third. We postulate that this incomplete attachment will only retain the intermediate for a very brief time (for example, less than 1 millisecond) before the latter breaks loose and diffuses elsewhere. However, when it eventually diffuses to the correct place, it will be held by hydrogen bonds to all three bases and will thus be retained, on the average for a much longer time (say seconds or minutes). (14)

This view suggests that even a single mismatch in the base pairing between tRNA and its template would give rise to differences in affinity of three to four orders of magnitude. At the time this was proposed, it was not even clear whether the template was DNA or RNA. Moreover, tRNA was thought to be able to diffuse freely along the template because the role of the ribosome was then unknown. Nevertheless, the adaptor hypothesis was confirmed soon afterwards by the discovery of tRNA (15) and its sequence (16), which suggested base pairing between a trinucleotide anticodon and the mRNA codon.

Conceptually brilliant as the adaptor hypothesis was, the reasoning above made no attempt to ask if the underlying chemical interactions would actually give rise to the stabilities desired. The estimates of lifetimes appear to have been simply made up. One of the first attempts to put the question of specificity in quantitative chemical terms was made by Pauling (17), who was troubled by the question of how two similar amino acids, valine and isoleucine, could be discriminated by the protein synthesis machinery. He proposed that there was an upper limit to the accuracy, based on the difference in the binding energy of each amino acid to

the discriminating enzyme, namely the aminoacyl synthetase that would charge the appropriate tRNA with an amino acid (17). Subsequent work on enzymes showed that if binding is followed by a catalytic step, the selectivity is related to the difference in the free energy of the transition state for the correct versus incorrect substrate. This quantity is more directly related to k_{cat}/K_m, a measure for the relative rates of incorporation of the correct versus the incorrect substrate (5).

Even to begin to understand the sources of translational fidelity, it is necessary to know, on the one hand, the overall in vivo accuracy of protein synthesis and, on the other, the free energy difference in base pairing between correct and incorrect tRNAs. One of the first quantitative estimates of missense errors during the synthesis of a protein was made by Loftfield (18), who measured the incorporation of specific labeled amino acids into defined proteolytic fragments of ovalbumin. Using five different peptides, Loftfield thus determined misincorporation rates for Ile, Val, and Leu, spanning a range of 2×10^{-3} to 7×10^{-5}, with a median value of 3×10^{-3}. As none of the separate steps of gene expression (transcription, tRNA-aminoacylation, and decoding) can be less accurate than the overall value, this also provided an estimate of the upper limit of the error rate of decoding. Because these rates were in fact comparable to the accuracy estimated for tRNA aminoacylation, it was even possible that the error rates of codon-anticodon pairing might be substantially lower. Among the amino acids considered, the codon-anticodon mismatch bearing the greatest similarity to cognate pairing was the potential binding of Ile-tRNA^{Ile} on Val codons with a G1:U base pair at the first codon position in the place of a standard Watson-Crick A1:U pair (in X*n*:Y, *n* refers to the base position in the codon). A similar (but symmetrically flipped) situation between the U1:G mismatch and the cognate U1:A pair applies to misincorporation of Leu in the place of Phe, for which Loftfield, on the basis of more tentative data, estimated a similar frequency. Such codon-anticodon mismatches are today referred to as near cognate (mismatches which differ more significantly from cognate are referred to as noncognate). Following the Watson-Crick model above, Loftfield concluded that the most evident basis for specificity appeared to reside, in some undefined manner, in the presence or the absence of individual, base-pairing hydrogen bonds. However, using Pauling's arguments, he argued that the differences in free energy of binding thus expected could hardly account for the high levels of discrimination observed. Thus, the decoding problem was recognized and clearly articulated as early as 1963.

Subsequent in vivo measurements again suggested error rates of around 10^{-3}–10^{-4} in various contexts (11, 19–21). Measurements using in vitro translation systems initially suggested much higher error rates, but it was found that the low temperatures and high levels of magnesium ions used artificially increased the error rates (22–24). Buffers that contained lower levels of magnesium but included polyamines, calcium, and nucleoside triphosphate regeneration gave error rates comparable to those obtained in vivo (25).

How do these values compare with the expected specificity of base pairing in solution? These values were difficult to measure initially, both because the

synthesis of defined oligonucleotides was technically difficult and the interaction between even fully complementary tri- or tetranucleotides is too weak to be studied (26). Equilibrium dialysis (close to the detection limit of the method, in the 0.1–1 M dissociation constant range) was used to measure the affinities between $tRNA^{fMet}$ and tri- or tetranucleotides containing the intiation codons AUG or GUG (27). The GUG codon with the G1:U wobble at the first codon position bound to a very similar level as the AUG codon with the A1:U codon-anticodon pair (relative GUG binding was about 70%, corresponding, at 0°C, to a loss of less than 0.8 kJ/mol in interaction energy).

Eisinger et al. (28) exploited a characteristic blue shift in fluorescence emission of the modified G (Y-base) at the position 3′ to the anticodon, which depends upon association with a codon, to measure the affinities of yeast $tRNA^{Phe}$ to its two cognate codons UUU and UUC (29). This measurement addressed the difference between the pairs U3:Gm34 and C3:Gm34 and showed that the "wobble codon" UUU binds $tRNA^{Phe}$ ~5 times more weakly than UUC. These values were confirmed by equilibrium dialysis measurements (30).

A different approach was used when it was discovered that two tRNA molecules with complementary anticodons could dimerize with an affinity that was up to six orders of magnitude stronger ($K_d \sim 10^{-6}$ M) than would be expected from normal trinucleotide associations (31). This enhanced stability is thought to arise primarily from helix-stacking effects and results almost entirely from a reduction in the dissociation rate (32). The formation of an extended helix by the two anticodon stems, which stack across the two anticodons, was confirmed by the crystal structure of the $(tRNA_{Asp})_2$ complex (33). This base-stacking effect also explains (32) why trinucleotides associate more strongly with a tRNA anticodon than with another complementary trinucleotide (26). A different kind of "stacking," by the hydrophobic modification of the purine 3′ to the anticodon (e.g., the Y base) was also shown to contribute significantly to the stabilization (about one order of magnitude).

Because the enhancement of affinity also applied to tRNA species with imperfectly paired anticodons, this system appeared to allow a more accurate and comprehensive study of the effect of mismatches within triplet pairs and was used as a model of the codon-anticodon interaction in the absence of the ribosome (34). Of necessity, the study had to combine tRNAs with nucleoside modifications at or near the anticodon in an unphysiological manner, and these modifications affected the dimerization stability at least as much as mismatches in the codon-anticodon pairs themselves. Additionally, the contributions of helix-stacking interactions could also vary considerably. Thus, although a phenomenon of some interest from the point of view of general nucleic acid chemistry, tRNA dimerization was not well suited as a model for studying the inherent specificity of base pairing.

Despite the fact that studies on tRNA-codon interactions (27, 29, 30) suggested a less than 10-fold reduction in affinity due to a G:U mismatch, the results on tRNA dimerization (34) led to a widespread notion in the literature on translational accuracy that mismatches differ from Watson-Crick pairs by "only 2–3 kcal/mol," e.g., Reference 35. This free energy difference $\Delta\Delta G^0$ (i.e., 8–13 kJ/mol;

1 cal = 4.184 J) could account for an error rate of about 1:100 rather than the <1:10 difference measured previously. This alleged value for the minimum inherent specificity of codon-anticodon interactions outside the ribosome has led to confusion about the ultimate source of tRNA discrimination by the ribosome, and resulted in a conclusion that the ribosome does not add to the inherent specificity of codon-anticodon base pairing over that in solution (36).

The thermodynamics of base pairing, and hydrogen bonding in general, are today quite well understood. Extensive melting studies have been carried out on defined oligonucleotides in order to derive thermodynamic parameters for all possible base pairs, in the contexts of all possible nearest neighbors (compiled data, for 37°C, e.g., in References 37–39). Generally, the immediately adjacent sequence neighbors account for the largest part of the (considerable) influence of the sequence context on the stability of a given base pair. Hydrogen bonding and base stacking contribute approximately equally to base pair stability, and the energetic contribution of a hydrogen bond to the stabilization of a base pair within a helix is on average 4 kJ/mol (40). This is therefore no different than, for example, in protein-ligand interactions or RNA tertiary structure, in which the energetic contribution of an uncharged hydrogen bond toward the total interaction energy usually varies between 2 and 6 kJ/mol (41–46).

The comparison of the stability of G:U wobble mismatches compared to A:U Watson-Crick pairs is of interest with regard to decoding. Accurate differentiation between these two base pairs is required (except at the third codon letter) by the genetic code in order to distinguish, e.g., Phe-tRNA^{Phe} from near-cognate Leu-tRNA^{Leu} and many other similar codon-anticodon combinations. However, in oligonucleotide helices, the stability of terminal G:U pairs can be approximately equal to A:U pairs (47, 48) or even slightly greater than that of A:U pairs when stacking on an adjacent Watson-Crick pair with "flipped" orientation of the purine and pyrimidine partners (39). This confirms the earliest thermodynamic comparison of G1:U to A1:U at the 5′ position of a trinucleotide codon binding to tRNA^{fMet} mentioned above (27). Internal G:U pairs are less stable than A:U pairs by an average factor of 0.3, corresponding to a loss in free energy of helix formation ($\Delta\Delta G^0$) of 2.9 kJ/mol at 37°C. Depending on sequence context, the factor of destabilization by internal G:U covers a range of 0.7 to 0.1 (49). Considering the in vivo error rates discussed above, it is clear that the specificity of base pairing by itself cannot account for the accuracy of tRNA selection. A free energy difference $\Delta\Delta G$ of 18–24 kJ/mol would be required to account for the error rates of 10^{-3}–10^{-4}, which are observed in translation, both in vitro and in vivo.

THE ROLE OF THE RIBOSOME IN DECODING

It was clear in the early 1960s that no trinucleotide association was stable above 25°C (50–52) and that the ribosome must stabilize this interaction, e.g., Reference 53. Crick had previously countered arguments that triplet interactions might

(generally) be too weak to account for the reading of the code by postulating that the codon and anticodon would interact in a "very special environment," in which a protein would "assist, unspecifically, in strengthening the binding of [t]RNA" (54). This view, namely that the ribosome merely strengthens the binding of tRNA but does not add to the specificity of the codon-anticodon interaction over what exists in solution, has persisted continuously in the literature until quite recently (e.g., Reference 36, and see below). Thus, although it was soon well accepted that the ribosome must stabilize tRNA binding overall (53), an unresolved issue in the four decades that followed has been whether this interaction applies equally to all aa-tRNAs, or whether the stabilization by the ribosome in fact also contains specificity for cognate codon-anticodon interactions.

Mutations and Antibiotics that Affect Translational Fidelity

The first indications that the ribosome might do more than nonspecifically increase the affinity of all tRNAs came from the realization that the fidelity of translation could be affected by both antibiotics that bind to the ribosome and mutations in the ribosome.

STREPTOMYCIN The discovery that streptomycin allows growth of certain auxotrophs, even in the absence of normally required nutrients, led to the idea that the antibiotic might induce mistakes in decoding (55, reviewed in 56, 57). In these auxotrophs, enzymes involved in the synthesis of required metabolites were defective because of premature stop codons in their genes. The presence of streptomycin leads to readthrough of these premature stop codons, allowing the production of functional protein and growth in the absence of the metabolite ("environmental suppression" of nonsense mutations). Parallel in vitro studies showed that streptomycin caused extensive misincorporation of incorrect amino acids not normally encoded by the template (22). This led to the proposal that the ribosome has a decoding site that somehow recognizes the codon-anticodon interaction, and streptomycin would affect this recognition.

Streptomycin-resistant (SmR) mutants also proved interesting. Whereas resistance is often acquired by preventing binding of antibiotics to their target by modification of either component, SmR mutants generally work by compensating for the effects of streptomycin. Thus, there were "conditionally streptomycin dependent" auxotrophic nonsense mutants of *E. coli* (55). These mutants displayed a streptomycin-dependent (SmD) phenotype in the absence of the metabolite they were unable to synthesize. Streptomycin was then required to allow enzyme production by readthrough of the nonsense mutations. Some of these nonsense mutations displayed a "leaky" readthrough at a low level even in the absence of streptomycin. However, mutations at the *strA* locus conferring resistance to or dependence upon streptomycin restricted this low-level readthrough. This locus was shown to correspond to the *rpsL* gene, which encodes the small ribosomal subunit protein S12 (58). In some of the restrictive SmR or SmD S12 mutants,

streptomycin restored translational leakiness. In others, the restrictive effect of the S12 mutation was so strong that addition of streptomycin had no effect.

These in vivo effects were soon correlated with the finding that ribosomes containing the SmR or SmD mutations in S12 also restricted the capacity of streptomycin to induce misreading in vitro (22), reviewed in (57). Furthermore, these mutations conferred hyperaccurate decoding properties upon ribosomes, preventing both missense errors and frameshifts (59), reviewed in (60). In one in vivo study on two particular codons in *E. coli*, an SmR mutation (in the absence of Sm) reduced overall translational missense errors to one third and one seventh of the wild-type level (11). Other error-inducing agents, such as paromomycin or even ethanol, could substitute for streptomycin in some SmD mutants (61).

RAM MUTANTS Mutants with decreased translational accuracy were isolated owing to their property of reversing the effect of restrictive mutations (62, 63). As second-site mutations, these so-called *ram* (ribosomal ambiguity) mutations remove the streptomycin-dependent phenotype in the restrictive background mentioned in the preceding paragraph (57, 64). *Ram* mutations of this type were mapped first to the small ribosomal subunit proteins S4 (65) and then to S5 (66, 67). *Ram* mutations enhance translational leakiness and suppression of nonsense mutations or restore these phenomena in a restrictive background, in a manner equivalent to Sm. Interestingly, the contributions of streptomycin and *ram* mutations toward the overall degree of "derestriction" (error-prone translation) are additive (68). The antagonistic relation between the *ram* and the S12 mutations was also true in the reverse situation: Introduction of a restrictive mutation of protein S12 into an error-prone *ram* background restored misreading to the low wild-type level (68).

MUTATIONS IN tRNA DISTANT FROM THE ANTICODON In the absence of a structure of the ribosome, it was not clear originally whether the restrictive and *ram* mutations were part of the decoding site. The discovery of a tRNA mutation that was demonstrably far from the anticodon loop and yet affected decoding was therefore both of great interest and a puzzle.

Apart from the effects of the aforementioned *ram* mutations, other instances of "genetic" nonsense (and missense) suppression were initially assumed to arise from alterations to the tRNA anticodon, conferring complementarity and, therefore, specificity to a stop codon (or a different sense codon). However, one UGA nonsense suppressor showed this need not always be the case (69, 70). In this so-called "Hirsh suppressor," a mutation at a quite distant site (G24A within the D arm of tRNA, see Figure 5 below) confers upon Trp-tRNA^{Trp} the ability to pair to the UGA codon with a normally forbidden A3:C codon-anticodon mismatch at the wobble position. It was later shown that this tRNA could also translate the UGU and UGC codons (71).

However, some tRNA species with directly altered anticodons do not efficiently read the codons that would have become cognate, see (57). Such observations indicated at an early stage that not only the codon-anticodon duplex and the ribosome,

but also the structure of the entire tRNA, must play an important role in the tRNA selection mechanism. This demonstrated that the wider structural context in some way governs the accessibility of productive, nonstandard pairing modes for the codon and anticodon. To explain this, Gorini (57, 72) attributed to the ribosome a mysterious "screening force" that would allow binding of tRNAs to the ribosome but prevent them from reaching the stage of codon-anticodon interactions. The selection of the tRNA would depend not only on the anticodon but also on other aspects of the tRNA and its interaction with the ribosome. How this screen might work in practice was never really clear.

Mutations that affect accuracy have since been found in many different parts of both subunits of the ribosome. Mutants of the 50S ribosomal subunit protein L7/12 that increased missense or nonsense suppression were isolated (73, 74). One of these mutants behaved very similarly to the S4 and S5 *ram* mutants in that it eliminated streptomycin dependence and also caused enhanced misreading in vitro. A large number of functionally related mutations have been isolated in the RNA of both ribosomal subunits as well as in EF-Tu. These mutations confer resistance to streptomycin or paromomycin and often to a hyperaccurate phenotype, or they increase misreading in vitro or in vivo, reviewed in (4).

Ribosomal Recognition of Base-Pairing Geometry

The work on antibiotics clearly showed that the ribosome directly affected the fidelity of translation. There were two lines of reasoning as to how this would occur. These two lines were thought of as opposing viewpoints, but as we shall discuss, this is not really the case. The model of a decoding site on the 30S subunit that recognizes codon-anticodon pairing (22) implied that the ribosome distinguished correct from incorrect base pairing in essentially the same way that enzymes discriminated between correct and incorrect substrates, by extensive interactions that depended on substrate geometry (75). The additional interactions made with the correct substrate would lead to an enhancement of specificity over that present in base pairing alone. In a further elaboration of this idea, it was proposed that the ribosome directly recognized the 2′ OH groups of the ribose of the codon when correctly base-paired (76).

However, these proposals were difficult to reconcile with the observation of mutations that affected translational fidelity but were known to be quite distant from the codon-anticodon helix or indeed even in the other subunit. Thus, geometric recognition came to be replaced with a different notion based on kinetics.

The Kinetic Proofreading Hypothesis

In an initial attempt to explain the antibiotic and mutational data, it was proposed that the tRNA selection process could be divided into two steps, an initial loose association between codon and anticodon, followed by a more stable association that leads to peptidyl transfer (77). The transition time to go from the loose to the stable state could be affected by antibiotics or mutations. However, this scheme

could not by itself explain why the normal ribosome was so much more accurate than what would be expected from base pairing in solution.

Two independent papers in the 1970s (78, 79) showed that if a selection step can be repeated multiple times in a process while separated by essentially irreversible steps, then for n such steps with a selectivity s for each step, the final selectivity could be as high as s^n. This general method for enhancing selectivity is referred to as "kinetic proofreading." A two-step proofreading scheme as applied to the ribosome is shown in Figure 1*a*. Aminoacyl tRNA is presented to the ribosome by the ternary complex of elongation factor Tu (EF-Tu) with tRNA and GTP. This binding of the ternary complex to the ribosome is reversible, and noncognate ternary complex usually dissociates at this stage. However, if the pairing to the codon is cognate, EF-Tu hydrolyses GTP while bound to the ribosome, and then EF-Tu dissociates both from tRNA and the ribosome. This stage of the mechanism represents a branch point for those tRNAs that have made it past GTP hydrolysis by EF-Tu: Either the aminoacyl end of the tRNA becomes available for peptidyl transfer, or the aminoacyl tRNA dissociates from the ribosome.

Thus, the two dissociation steps for tRNA are separated by GTP hydrolysis. The overall selectivity is enhanced because the tRNA must pass unidirectionally and without dissociating through both selection steps in order to take part in protein synthesis. GTP hydrolysis on the ribosome can be considered irreversible because in the cell the GTP/GDP ratio is displaced far from equilibrium (80). Also, after GTP hydrolysis, the dissociation of free (i.e., non-EF-Tu-bound) aminoacyl tRNA is essentially irreversible, so that the tRNA cannot bypass the first selection step. This is because the cellular concentration of free aminoacyl tRNA is quite low, partly because of the high concentration of EF-Tu, and also because EF-Tu-mediated binding of aminoacyl tRNA to the ribosome is much more efficient than the factor-free association of charged or uncharged tRNA.

Evidence for the proofreading hypothesis came when it was shown that incorporation of near-cognate amino acids resulted in a 10-fold increase in GTP consumption by EF-Tu per amino acid (35). Noncognate amino acids, which could be efficiently rejected at the first step on base-pairing considerations alone, did not stimulate GTP consumption. These results were criticized on the grounds that they were done in nontranslocating in vitro systems and were based on the assumption that peptidyl transfer was irreversible, but experiments done in translocating systems showed that, if anything, an even higher (50-fold) increase in GTP consumption per near-cognate amino acid incorporated was observed (81). Interestingly, the additional GTP consumption for near-cognate tRNAs was reduced in the presence of streptomycin (82, 83), which at the time led to the notion that streptomycin affected the proofreading step. These experiments provided strong evidence that proofreading occurred in tRNA selection.

In the original version of the proofreading scheme, selectivity arose solely from differences in the dissociation rates of cognate and near-cognate tRNA. The association rates as well as the other processes, such as GTP hydrolysis and peptidyl transfer, were thought to occur at the same rate for both. In this view, EF-Tu

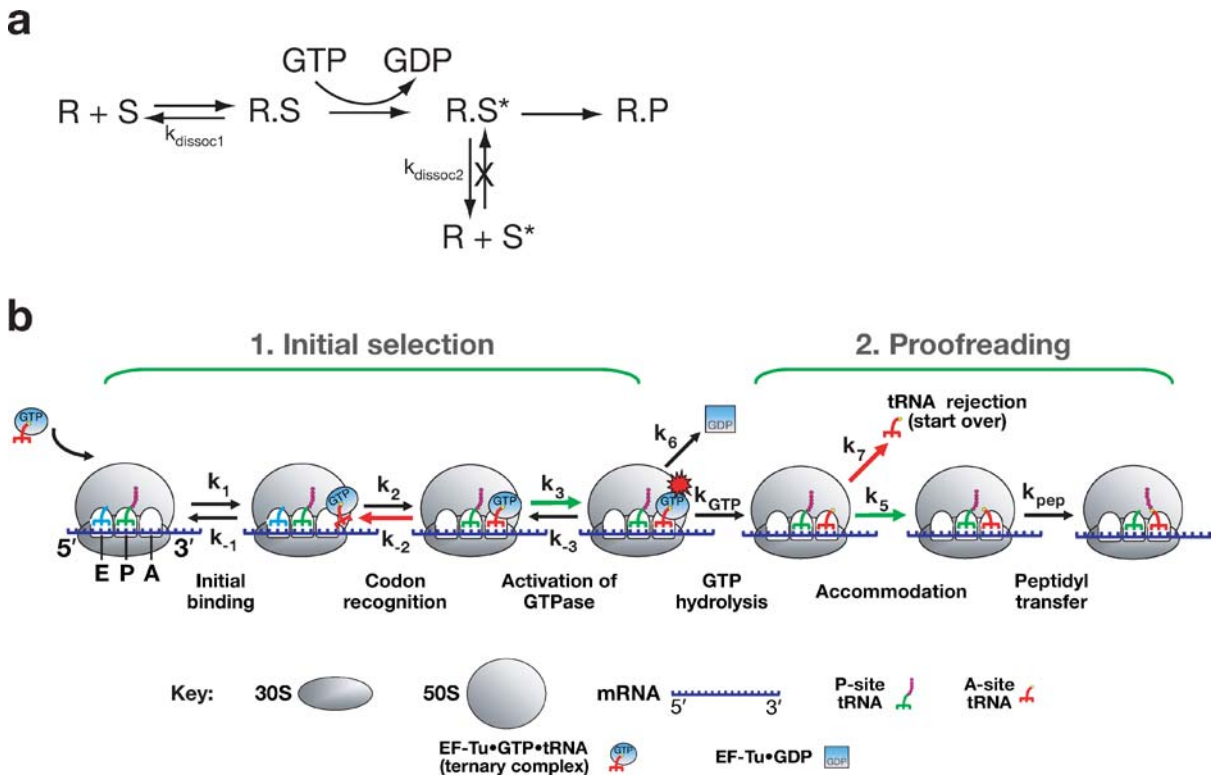

Figure 1 (*a*) The two-step kinetic proofreading scheme as applied to the ribosome. Here, R represents the ribosome, S the aa tRNA complexed with EF-Tu, and S* the aa tRNA alone. P represents the tRNA after peptide bond formation. (*b*) A tRNA selection scheme based on presteady-state kinetic data (91, 92). Red arrows show rates that are higher for near-cognate tRNA, whereas green ones show those that are higher for cognate tRNA.

acted as an internal clock, providing a delay between the binding of tRNA and GTP hydrolysis (84). Mutants that delayed the clock resulted in greater accuracy by allowing the tRNAs to equilibrate more fully at each step. Similarly, other mutations might speed up the clock. In accordance with this notion, the use of GTP-γS, a slowly hydrolysable analog of GTP, showed that, under near-equilibrium conditions, dissociation constants for cognate and near-cognate ternary complex differed by a factor of greater than 2000 or far in excess of the factor of 100 thought to be the intrinsic difference from base pairing at the time (85). How the ribosome would confer such an additional selectivity was never made clear, but it was suggested that the high selectivity was sacrificed for the sake of speed.

In the context of the simple scheme shown in Figure 1*a* that was known at the time, it was not clear how proofreading could work. As has been succinctly pointed out (86), cognate tRNA was thought to dissociate from the A site of the ribosome on a timescale of hours, whereas peptidyl transfer occurred in milliseconds. Thus, for proofreading to be effective, near-cognate tRNA would need an off rate that was 10^6 greater than cognate tRNA, which would eliminate the need for proofreading in the first place. Possibly such considerations led to the proposal that proofreading plays almost no role in tRNA selection. Therefore, in an alternative view, the occupancy of the E site with tRNA would lead to a reduced affinity for the A site (87, 88). This reduction in affinity was thought to come about mainly because of the loss of nonspecific tRNA-ribosome interactions, thus increasing the relative contribution of codon-dependent ones and, thereby, the capacity of the ribosome to discriminate between tRNAs on the timescale required. In this scheme, incorrect tRNAs would be more likely to dissociate (owing to the reduced affinity) prior to GTP hydrolysis. However, those who felt the ribosome could dispense with proofreading altogether by a purely geometric recognition had no good explanation for the experimentally observed excess GTP consumed for incorporation of a near-cognate tRNA. It was not until the use of presteady-state kinetics to dissect the various steps involved in tRNA selection that these paradoxes began to be resolved (36).

A Kinetic Scheme for tRNA Selection

In presteady-state kinetic experiments, molecular probes are used to report on various processes during a single turnover of ternary complex with ribosome. Such data are then combined and analyzed in terms of a kinetic model for the aa-tRNA selection pathway by numerical integration and global regression to determine a set of elemental rate constants describing both the data and the model.

Proflavin, incorporated at positions 16 or 17 in the D loop of yeast $tRNA^{Phe}$ (Figure 5), yields characteristic fluorescence signals upon EF-Tu:GTP-dependent binding to programmed *E. coli* ribosomes, which can be observed by single-turnover stopped-flow measurements (89). A small initial increase in the proflavin fluorescence is observed on binding of ternary complex to the ribosome, but this binding is not codon-dependent because it occurs with noncognate tRNA. A subsequent major increase in fluorescence is attributed to codon recognition since it is

not observed if the codon-anticodon pair is noncognate. The subsequent decrease in fluorescence is attributed to the accommodation (movement) of the aa-tRNA into the 50S A site and peptidyl transferase center. A second reporter in the tRNA is the blue shift in the fluorescence of wybutine (the Y-base of wybutosine, yW, which is a hypermodified derivative of G) at position 37, 3′ to the anticodon. This change in fluorescence reports more directly on codon-anticodon pairing. It is observed even when a trinucleotide binds the anticodon in the absence of the ribosome (28) and is due to stacking effects within and around the codon-anticodon duplex. The fluorescent signal from mant-dGTP, a GTP analog that is compatible with normal EF-Tu function (90), reports on the environment of the GTP-binding site in EF-Tu. Finally, the rate of GTP hydrolysis or peptide bond formation can be determined directly by quench-flow experiments using radioactively labeled substrates. To further dissect the various steps by blocking or slowing down the process at various stages, a number of devices, such as mutant factor, the antibiotic kirromycin, or nonhydrolysable analogs of GTP, were used.

Using data from these reporters, Rodnina and coworkers (91) were able to extend and add detail to the kinetic scheme for aa-tRNA selection at the ribosomal A site, as shown in Figure 1*b*. Elemental rate constants for the various steps were determined using global fitting for both cognate yeast Phe-tRNA^{Phe} (91) and for near-cognate Leu-tRNA^{Leu2} with the codon-anticodon mismatch U1:G (92) (Table 1).

The initial selection phase begins with a codon-independent and reversible rapid initial binding of the ternary complex (k_1, k_{-1}). This is followed by a step attributed to "codon recognition" (k_2, k_{-2}) in which the tRNA anticodon associates reversibly with the codon in the 30S A site (while the aminoacyl acceptor end is still bound to EF-Tu). Recognition between the cognate codon and anticodon leads to the stabilization of the ternary complex on the ribosome and the transmission of an activating signal to EF-Tu (GTPase activation, k_3), which is then stimulated to hydrolyze GTP (k_{GTP}). This activation signal is distinct from GTP hydrolysis or codon recognition since it occurs even with nonhydrolysable analogs, and it was possible to separate it from codon recognition in an EF-Tu mutant (93). After release of inorganic phosphate (k_{Pi}), EF-Tu rearranges into the GDP-bound conformation (k_4) (94–96), which dissociates from the aminoacyl end of aa-tRNA and the ribosome (k_6). The aa-tRNA is then at the proofreading branch point: Either the aminoacyl end of tRNA moves into the A site of the 50S subunit (accommodation, k_5), which leads to formation of the peptide bond (k_{pep}), or the aa-tRNA dissociates from the ribosome (rejection, k_7). Again, accommodation is a distinct step from peptide bond formation.

A striking finding in the comparison of cognate and near-cognate tRNAs was that, in addition to the expected difference in dissociation rates (k_{-2} and k_7, respectively, in the initial selection and proofreading steps), the forward rates of GTPase activation (k_3) and accommodation (k_5) were greatly accelerated for cognate in comparison to near-cognate tRNA. This led to a fundamental revision of the tRNA selection model, compared to the "internal kinetic standard" concept

TABLE 1 Elemental rate constants for tRNA selection by the ribosome

Step		Rate constants (s^{-1})					
		Cognate (5 mM Mg)[b]	**Cognate (10 mM Mg)[b,c]**	**Near-cognate (10 mM Mg)[c]**	**Near-cognate + Paromomycin (10 mM Mg)[d]**	**Cognate (optimized buffer)[e]**	**Near-cognate (optimized buffer)[e]**
Initial binding	k_1	60 ± 10	110 ± 10	110 ± 10	140 ± 20	140	140
	k_{-1}	30 ± 5	25 ± 5	25 ± 5	25 ± 10	85	85
Codon recognition	k_2	80 ± 10	100 ± 15	100 ± 20	37 ± 2	190	190
	k_{-2}	2 ± 0.5	0.2 ± 0.1	17 ± 8	3.5 ± 0.5	0.23	80
GTPase activation and GTP hydrolysis[a]	k_3	55 ± 15	500 ± 100	50 ± 20	>500	260	0.4
GTP-GDP conformational change in EF-Tu	k_4	60 ± 20	60 ± 20	50 ± 20	6 ± 2		
aa-tRNA accommodation and peptide bond formation[a]	k_5	8 ± 1	7 ± 2	0.1 ± 0.03	1 ± 0.1		
Dissociation of EF-Tu·GDP	k_6	4 ± 1	3 ± 1	2 ± 1			
aa-tRNA rejection	k_7		<0.3	6 ± 1	0.9 ± 0.2		

[a]Steps combined because the first is rate-limiting and the second is very rapid.
[b–e]Compiled from References [b](91), [c](92), [d](107), [e](97).

proposed a decade earlier (84). In the new scheme, substrate selection occurs not only because of differences in dissociation rates, but also, or even mainly, because of the kinetic partitioning of the cognate aa-tRNA toward formation of the peptide bond by acceleration of the forward reaction rates. It was proposed that the binding of cognate tRNA induces rate-limiting conformational changes that are required for the (otherwise inherently rapid) chemical steps of GTP hydrolysis or peptide bond formation (92). As discussed below, paromomycin and streptomycin affect the same forward rates affected by cognate tRNA. Moreover, the realization that accommodation was a rate-limiting step before peptidyl transfer meant that some of the classical objections to proofreading discussed in the previous section no longer applied.

It is always difficult to evaluate how close these estimated constants are to the values in vivo. In the original set of experiments that compared cognate with near-cognate tRNA (91, 92), a magnesium concentration of 10 mM and the relatively low temperature of 20°C were chosen in order to obtain measurable signals, especially for the incorporation of the amino acid into peptide in the near-cognate case. Under these conditions, the overall accuracy is highly compromised; in particular, there is almost no selectivity in the initial selection step (92). However, these concerns were addressed more recently using buffer systems that yielded a much higher overall accuracy that approaches those estimated in vivo (Table 1) (97). The results showed a much greater selectivity in the initial selection step, in which the acceleration of forward rates played a major role in selection of tRNA, as previously proposed. However, the estimated proofreading factor of 15 was significantly less than estimated in some previous studies, and the relative rates of accommodation for cognate and near-cognate tRNA were not reported, presumably because the accuracy limited the signal from near-cognate tRNA in the proofreading steps.

STRUCTURAL INSIGHTS INTO DECODING

The genetic and biochemical work described above clearly implicated the ribosome as having an active role in the decoding process. Elucidation of the structural aspects and the mechanisms underlying decoding proved to be more difficult until recently.

Over three decades ago, it was shown that modification of 16S RNA by kethoxal abolished binding of tRNA to the ribosome (98). At the time, even the sequence of 16S RNA was unknown. Much later, the development of base footprinting techniques showed that the 16S RNA bases G529, G530, A1492, and A1493 were strongly protected against chemical modification by the binding of A-site tRNA (99). In subsequent experiments, G530 (100) as well as A1492 and A1493 (101) were shown to be required for viability and for tRNA binding. Early on, G530, part of the "530 pseudoknot" in the 5′ domain of 16S RNA, was thought to be at some distance from the decoding site near A1492 and A1493 in the 3′ minor domain; its involvement was thought to involve a long-range allosteric interaction

(100). As we discuss below, crystal structures of the ribosome show that all three bases are in fact located in close proximity.

Paramomycin, which causes miscoding, was shown to protect A1408, G1419, and G1494, which are close to some of the bases protected by A-site tRNA (102). These bases are part of an internal loop in helix 44, which is the long penultimate helix in 16S RNA. An important finding was that an oligonucleotide encompassing this region could bind paromomycin in isolation (103). This paved the way for structural studies on this small fragment of 16S RNA by NMR in the presence (104) and absence (105) of paromomycin. Together, they provided the first three-dimensional information about the interaction and effects of an antibiotic bound to its RNA target site on the ribosome. As might have been expected from the footprinting and biochemical studies, paromomycin made extensive interactions with the internal loop containing A1492 and A1493. Comparison of the structures with and without paromomycin showed a modest displacement of A1492 and A1493 into the minor groove of helix 44, leading to the proposal that the antibiotic induces local conformational changes in the decoding site that would mimic the tRNA-bound conformation. This prediction turns out to be remarkably accurate, but oddly enough, the data on which it was based, namely the limited conformational changes seen in the NMR structure, did not reveal the role of A1492 and A1493 in decoding when crystal structures of the 30S subunit and the 70S ribosome emerged (see below).

In the absence of a structure for the 30S subunit, it was not clear whether paromomycin would work by inducing a conformational change to a tRNA-bound form as proposed above, or whether it would simply stabilize tRNAs (including near-cognate tRNAs) by making additional interactions with them (106). However, direct kinetic measurements showed that paromomycin accelerated the forward rates of GTPase activation and accommodation of near-cognate tRNA (Table 1) (107). These data were more easily reconcilable with the idea that paromomycin worked by inducing a conformational change to a productive form of the ribosome, similar to that induced by cognate tRNA.

These questions regarding paromomycin were related to a fundamental issue that remained open in the absence of direct structural data: Did the ribosome directly contact the codon-anticodon base pairs, and if not, were they sensed in some indirect way? Footprinting and genetic data are amenable to either interpretation. It was shown that the mutation of A1492 and A1493 to G would abolish A-site tRNA binding in the presence of mRNA (101), strengthening evidence for their involvement in tRNA recognition that was implied by earlier footprinting studies (99). In these mutant ribosomes, the presence of mRNA containing fluorine instead of an OH at the 2′ position on the ribose partly restored tRNA binding (101). This was interpreted to mean that the 2′ OH group of mRNA in the codon made a direct interaction with the N1 of A1492 or A1493. Because the N1 in a guanine is a proton donor rather than acceptor, it could not interact in the same way as the adenine with the 2′ OH of mRNA, but it might be able to do so if the group was changed to 2′ F, which is a proton acceptor. This led to the proposal that A1492 and

A1493 interact directly with the mRNA in the codon-anticodon helix and would sense the shape of the base pairs. However, the interaction of the N1 of A1492 and A1493 with mRNA, around which this proposal is constructed, is incompatible with what we now know on the basis of the crystal structure of the 30S subunit: The N1 of the conserved adenines interacts with the tRNA. It is their 2′ OH group (which is unchanged in a guanine) that interacts with mRNA. The structural basis for the data of the 2′ fluorine substitution experiment thus remains unclear. Therefore, the postulate, in very general terms, of a direct interaction between the two conserved adenines and the mRNA appears to have been only fortuitously correct, and the experiment upon which it is based cannot be considered proof for direct recognition of base-pairing geometry in decoding.

Crystallography of the Ribosome

It had become abundantly clear that many of the uncertainties and controversies about decoding could only be addressed in the context of a high-resolution structure of the ribosome or at least the 30S subunit. Over two decades ago, the 50S subunit was crystallized by Yonath, Wittmann, and their coworkers (108). Crystals of the 30S subunit and the whole 70S ribosome were originally reported by the Puschino group (109) and subsequently similar crystals of the 30S subunit were obtained by Yonath and coworkers (110, 111). Almost a decade of work by Yonath and coworkers resulted in improved crystals of the 50S subunit that diffracted to 3 Å resolution, raising the possibility that an atomic structure of it might one day be obtained (112). For almost a decade after crystals of the 50S were shown to diffract well, there were no comparable crystals of the 30S subunit or the 70S ribosome. In the late 1990s, two groups independently obtained improved crystals of the 30S subunit (113, 114). The diffraction limit of the 70S was also improved by the use of defined mRNA and tRNA as ligands (115).

Although well-diffracting crystals of the 50S subunit were reported in 1991, the phase problem for such large asymmetric objects remained intractable for many years. The first clear demonstration that reliable low-resolution phases could be obtained for ribosome-sized asymmetric units occurred when it was shown that peaks from heavy-atom clusters could be seen directly in difference Patterson maps of data from the 50S subunit, and right-handed helices of RNA were visualized in the electron density maps (116).

In 1999, a breakthrough was made in the crystallography of ribosomal subunits and the whole ribosome when the subunits were solved to resolutions of 5–5.5 Å (114, 117), which allowed placement of proteins of previously known structure into maps of the whole subunit as well as identification of stem-loops of parts of ribosomal RNA. This was soon followed by a structure of the whole ribosome complexed with mRNA and tRNA to 7.8 Å resolution (115). In the following year, 2000, complete atomic structures of the 30S subunit, from the Medical Research Council (MRC) group, (118) and the 50S subunit (119) were published. At the same time, an independent 30S subunit structure was solved to somewhat lower resolution

by the Max Planck/Weizmann group (120), but because it was incomplete in its tracing of the proteins and had significant errors in both the registry of the RNA and the topology of many of the previously unknown proteins, it has not proved as useful. Of particular relevance to decoding is that in the Max Planck/Weizmann structure, S12 was not built into sequence, was incomplete, and had incorrect topology. A more detailed comparison of the two original 30S structures has been published (121), and structures of the 30S subunit published the following year by the Max Planck/Weizmann group (122) are essentially in agreement with the MRC structure published originally. The year 2001 also saw the publication of the structure of the whole 70S ribosome complexed with mRNA and tRNA at a resolution of 5.5 Å (123). This structure relied for its molecular interpretation on the previously solved atomic structures of both subunits and the known structure of tRNA, but nevertheless, this was a major advance because it positioned the tRNA ligands in the context of the whole ribosome and provided an idea of the intersubunit contacts.

These structures made clear the environment of tRNA in the A site of the 30S subunit. The A site consists of a pocket formed by the 530 loop in the 30S body, a portion of the long helix 44 that lies along the subunit interface, and helix 34 from the 30S head domain (Figure 2*f*). In particular, the conserved bases G530, A1492, and A1493 line the floor of the A site, with C1054 from the head close by. Interestingly, the only protein in the vicinity of the A site is S12, which contains the sites of a number of fidelity mutations.

Initial Insights from Crystal Structures

In the 7.8 Å structure of the ribosome with bound A-site tRNA, it appeared that A1492 and A1493 were 15 Å away from the codon-anticodon helix, and it was

Figure 2 Recognition of the codon-anticodon helix by the ribosome. Panels (*a–c*) show the first–third base pairs, respectively, between a UUU codon and the cognate GAA anticodon from the Phe anticodon stem-loop (ASL). Ribosomal elements closely interact with the minor groove at the first two base pairs but less so at the third (wobble) base pair. (*d*) Interactions at a UG mismatch from a Leu near-cognate ASL at the first codon position. The cognate UA base pair is shown for comparison. (*e*) Structure of a UG mismatch from a Ser near-cognate ASL, showing Watson-Crick geometry and, thus, implying an unusual tautomer for the U or G. The electron density observed is shown, and the alternatives for the U or G represent their putative locations if the UG pair had standard wobble geometry and either the U or the G were positioned in the electron density. (*f*) Ribosomal environment at the decoding center with codon, cognate ASL, and paromomycin. The three bases G530 (*turquoise*), A1492, and A1493 (*cyan*) line the minor groove of the codon-anticodon helix at the center of the figure. The position of streptomycin is from (124). Reproduced with permission from (128) (*a–c*), (132) (*d–e*), and (147) (*f*).

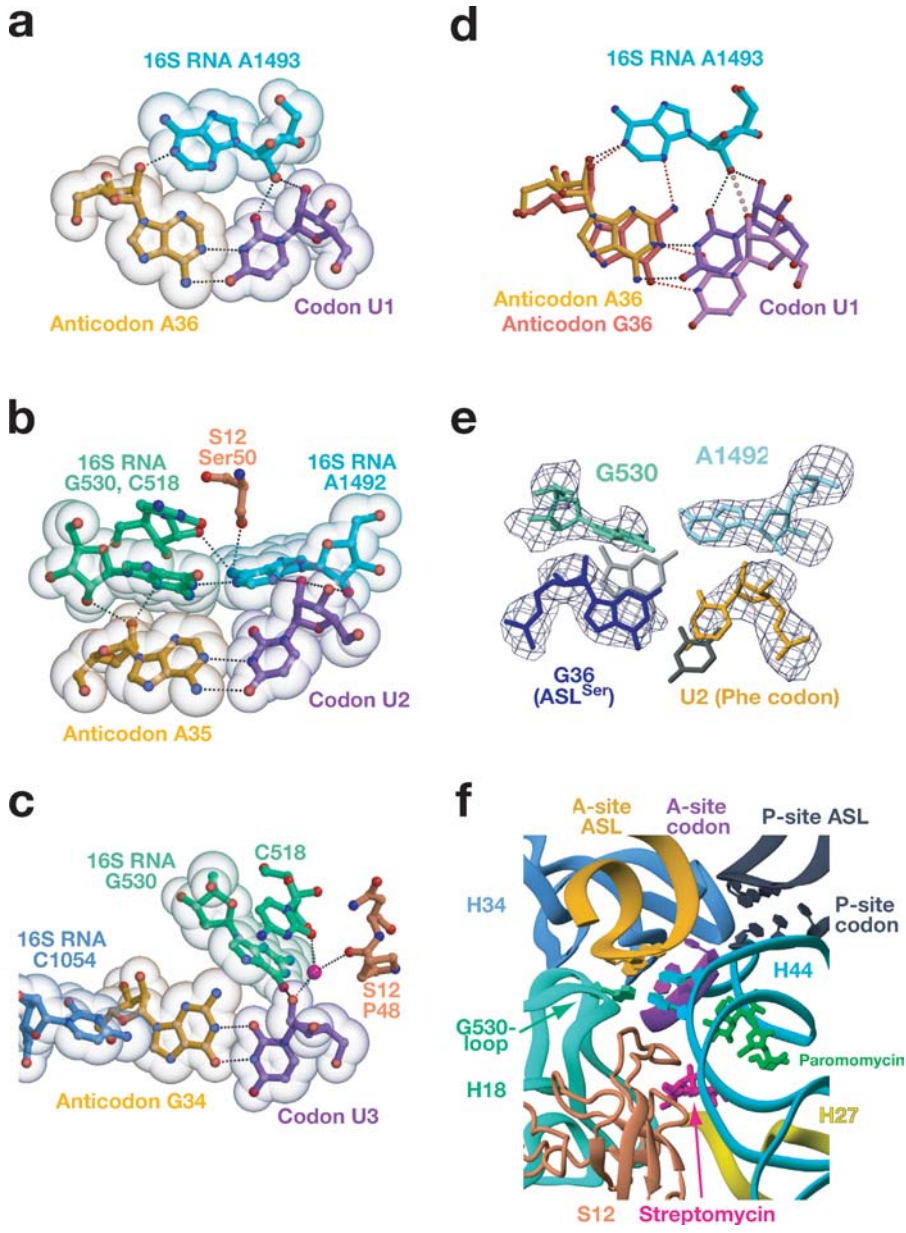

therefore concluded that they were unlikely to have a direct role in decoding (115). At that resolution, however, the conformation of these bases could not be determined. Furthermore, in this structure the occupancy of the tRNA was rather low (25%) (123), possibly because that crystal form could not accommodate the conformational changes that occur upon A-site binding (see below). Nevertheless, when the atomic structure of the 30S subunit was solved, a superposition of the A-site tRNA from the low-resolution 70S structure also suggested that the adenines in the unliganded 30S structure were too far away to make contact with the codon or anticodon in the A site (118). This remained true even when the NMR structure of the complex of paromomycin with the fragment of helix 44 containing A1492 and A1493 (104) was placed into the 30S subunit structure. The modest displacement of these bases induced by paromomycin in the NMR structure still left them too far away to make contact with the codon-anticodon helix. Therefore, it appeared initially that these bases had no direct role in sensing the codon-anticodon helix.

The matter remained unclear until the structure of the 30S subunit complexed with the antibiotics paromomycin, streptomycin, and spectinomycin was determined (124). Paromomycin, with a conformation similar to that in the previous NMR structure, was located in the internal loop of helix 44 (104), but the bases A1492 and A1493 were now completely displaced out of the loop and pointed into the A site. In particular, the structure was incompatible with a base pair between A1408 and A1493 that was observed in the NMR structure of the helix 44 fragment. Superposition of the tRNAs from the low-resolution 70S crystal structure suggested that, in this conformation, the bases could make direct contact with the minor groove of the codon-anticodon helix. It was therefore proposed that these adenines could directly read the geometry of the codon-anticodon base pairs. The crystal structure thus supported the idea that paromomycin would induce a tRNA-bound conformation in the 30S subunit, as suggested earlier (105) and as implied by kinetic data (107).

It remains unclear why the conformation of A1492 and A1493 differs in the crystal structure of the 30S subunit with paromomycin (124) and in the NMR structure of the corresponding fragment of 16S RNA complexed with paromomycin (104). The conformation of these bases in a crystal structure of a similar fragment of 16S RNA with paromomycin (125) is very similar to that in the crystal structure of the 30S subunit and unlike the NMR structure. Recently, the reasons for this difference were explored in a reanalysis of the NMR data (126), and it was concluded that the NMR structure, with the A1408–A1493 base pair, was in fact consistent with the data. Thus, the differences between the NMR and crystal structures are real. It has been suggested that the crystal structure represents the end point conformation of the paromomycin complex and that at physiological temperature the adenines would be dynamic (126). This is unlikely because, in general, flash cooling of crystals traps the variety of conformational states present, as judged by the high temperature factors of loops and other disordered regions—even in crystals studied at 100 K. In the free 30S structure, the conformational mobility of these adenines can indeed be inferred from the very high temperature factors (118), but

this mobility appears to be dramatically reduced in the presence of paromomycin. It was also argued (126) that in the crystal structure of the fragment of 16S RNA with paromomycin (125), the adenines are stabilized in the flipped-out form because they make minor groove interactions with a neighboring helix in the crystal lattice. However, this is not the case for the 30S subunit structure. A plausible explanation for the difference between the crystal and NMR structures is that in the 30S subunit, the presence of paromycin also induces additional interactions between protein S12 and the phosphate backbone of helix 44 (at 1492), which may stabilize the flipped-out conformation of the adenines. It should be remembered that the A site is not just a portion of helix 44 but the entire binding pocket for tRNA, including the 530 loop, portions of the head, and, more indirectly, protein S12 (see below). The crucial difference in the conformation of these adenines in the NMR and crystal structures is therefore an example of the limitations of studying a fragment out of context.

Structures of the 30S Subunit with Codon and Anticodon Stem-Loops in the A Site

The structure of the 30S subunit with paromomycin was suggestive, but a conclusive demonstration of how codon-anticodon base pairing is monitored had to await direct structural visualization of these interactions. Fortunately, when 30S subunits are crystallized in their native form, the A site remains accessible to relatively large ligands by diffusion, as was first demonstrated for initiation factor 1 (127). Thus, oligonucleotides corresponding to mRNA and a tRNA anticodon stem-loop (ASL) were soaked into crystals of the 30S subunit, and visualized at the 30S A site in difference Fourier maps (128). In this initial study, a U6 hexanucleotide, which places the UUU codon for phenylalanine in the A site, was studied along with its cognate ASL^{Phe}, both in the presence and absence of paromomycin. In addition, a structure was determined with paromomycin alone rather than with the combination of the three antibiotics paromomycin, streptomycin, and spectinomycin previously studied (124).

Both global conformational changes, indicating a domain closure of the 30S subunit around the ASL and local conformational changes in the decoding site, were observed. The significance of the global conformational changes were not immediately clear. However, it was obvious that the presence of a cognate codon-anticodon helix in the A site induced a change in the conformation of A1492 and A1493 to one which was similar to that seen with paromomycin, either alone or in the additional presence of streptomycin and spectinomycin. In the native structure (3.05 Å resolution), these adenines are highly disordered with B factors of 179 $Å^2$ and 201 $Å^2$, respectively. In the structure with paromomycin (3.3 Å resolution), these are reduced to 139 $Å^2$ and 94 $Å^2$, whereas in the structure with paromomycin, streptomycin, and spectinomycin (3.0 Å resolution), they have B factors of 90 $Å^2$ and 83 $Å^2$, respectively. The biggest drop is in the presence of cognate codon-anticodon pairing (3.3 Å resolution, without paromomycin) when

the corresponding B factors are reduced to 61 $Å^2$ and 43 $Å^2$. This suggests that both paromomycin and the codon-anticodon helix stabilize the adenines in a conformation in which they are displaced into the A site, but this must be regarded more as a restriction of conformational flexibility rather than a flip as originally described.

The term flip is, however, better used to describe the mechanistic action of G530, which was finally clarified by these structures: The guanine base ring, which is in a *syn* conformation in both the native and the antibiotic bound 30S structures, rotates into an *anti* conformation in the presence of the codon-anticodon helix. The result is that the three bases, G530, A1492, and A1493, make extensive interactions with the minor groove of the codon-anticodon helix (Figure 2). A1492 thereby also directly interacts with G530 as well as protein S12. Thus, the shoulder domain (S12 and the G530 loop) becomes connected directly via the codon-anticodon duplex to the 16S RNA helix 44 at the decoding center, resulting in a global "domain closure" of the 30S shoulder (Figure 3).

Various theoretical models were previously proposed for the interaction of ribosomal bases in the decoding center, which differ from the actual structure in the following ways: The N1 of these adenines interact with the 2′ OH of tRNA or with the N1 of G530, rather than with the 2′ OH groups of mRNA as inferred on the basis of biochemical experiments discussed above (101). The structure also does not support a model in which the N6 of these adenines forms a hydrogen bond with the O2 of pyrimidines or N3 of purines on mRNA (106). The closest prediction was based on the 30S structure complexed with paromomycin (and streptomycin and spectinomycin), namely that A1492 and A1493 would flip out of helix 44 to recognize the minor groove of the codon-anticodon helix (124) and thus discriminate between Watson-Crick and noncanonical pairs. However, examples of how this might occur were drawn from tertiary interactions found elsewhere in the structure of 16S RNA, wherein the adenines bind the minor groove in either an N1-N6-N7 or an N1-N6-N3 mode. But in fact, the orientation of these adenines and the principles of the codon-anticodon pairing specificity are different and involve neither the N6 nor N7 atoms of A1492 or A1493.

Instead, A1493 and A1492 adopt what have since come to be known as type I and type II A-minor motifs, respectively (129, 130). These tertiary interactions are often found with pairs of consecutive adenines and the minor groove of a nearby helix of double-stranded RNA, and they are found in both 16S and 23S RNA as

Figure 3 Domain closure in the 30S subunit induced by cognate tRNA binding, indicated by red arrows. (*a*) Overview of 30S elements involved in decoding. (*b*) A schematic diagram illustrating the relationship between domain closure (shoulder movement) and elements in the 30S subunit that affect translational fidelity. The view shows a cross section through the 30S subunit indicated by the plane in (*a*). Reproduced with permission from (147).

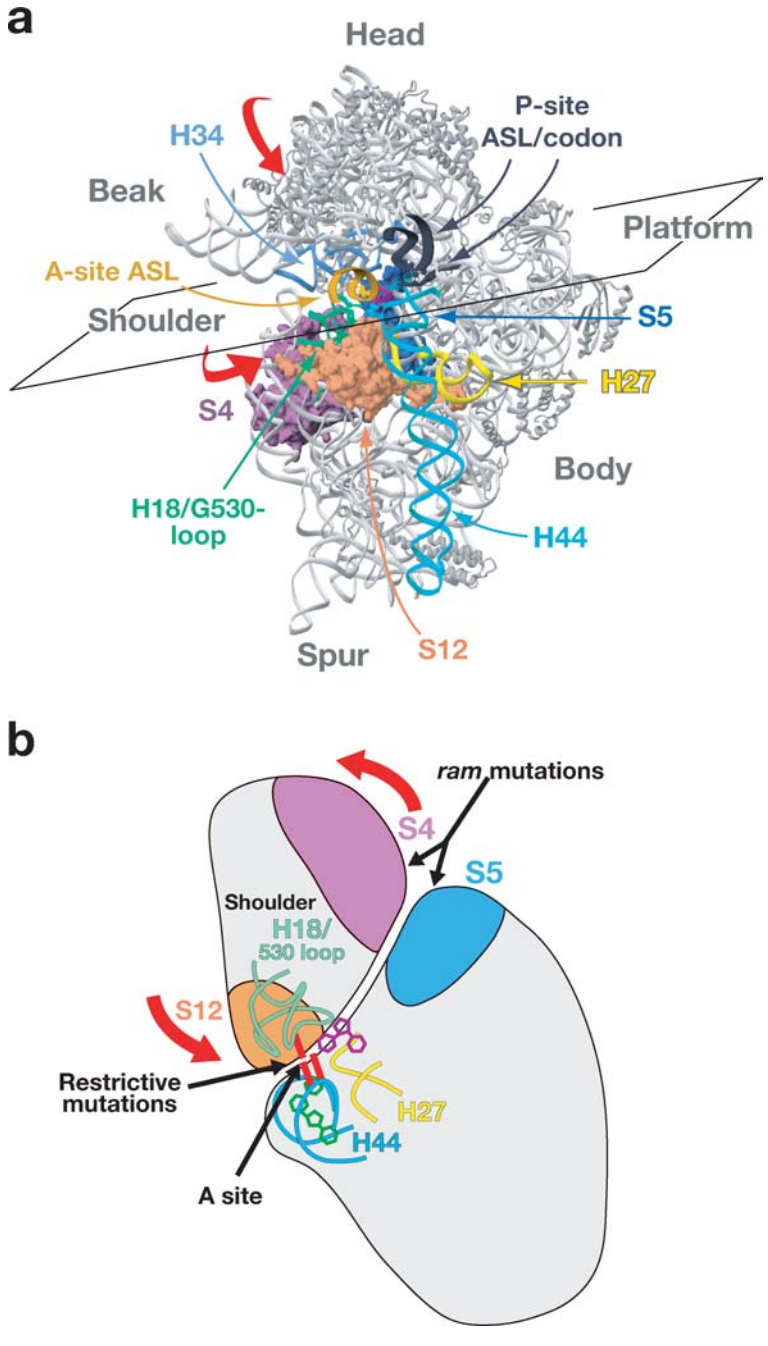

well as in the group I intron. In the case of the type I A-minor motif adopted by A1493, the adenine spans the minor groove, and the nucleotide makes contacts with both the codon and anticodon strands. There are hydrogen bonds between the 2′ OH of A1493 and both the 2′ OH and the O2 of a pyrimidine (or the N3 of the purines) in the codon, and the N1 of the adenine makes a hydrogen bond with the 2′ OH of tRNA. In contrast, A1492 forms a type II A-minor motif, which does not span the entire minor groove but only half of it, and makes hydrogen bonds to the codon nucleotide 2′ OH with both its N3 and its 2′ OH. In most tertiary interactions involving such pairs of consecutive A minor motifs, this second adenine makes hydrogen bonds with water molecules that act as a bridge to the strand on the other side (125), but in the ribosome, it is G530 that fills the rest of the minor groove.

The interactions of the ribosome with the codon-anticodon helix help us understand a long-standing and puzzling feature of the genetic code: The ribosome makes intimate contact with the minor groove at both the first and second positions in a way that is dependent on Watson-Crick base-pairing geometry (Figure 2*a*,*b*). In contrast, at the third (or wobble) position, only G530 contacts the 2′ OH of the codon nucleotide and the N2 of the anticodon guanine, in a way that appears to be relatively insensitive to the shape of the minor groove (Figure 2*c*). In particular, in the case of the ASL^{Phe} studied, the third position has the classic U·G wobble pair, which is readily accommodated. These results suggest that the ribosome closely monitors the geometry of base pairing at the first two positions but not at the third position, which would rationalize in structural terms why noncanonical base pairs are permitted at the third position in a codon but not the first two.

Work on the type I A-minor motif from the group I intron suggests that the free energy difference $\Delta\Delta G$ between interaction of the adenine with the minor groove of a Watson-Crick base pair, as compared to a wobble G·U or U·G pair, can be as much as 16–40 kJ/mol (4–10 kcal/mol), which corresponds to an affinity ratio of 10^4 (131). The occurrence of the same type I A-minor motif at the first codon-anticodon base pair suggests that the minor groove interaction alone can differentiate sufficiently between Watson-Crick and wobble pairs to account for the accuracy of translation. Superficially, this appears to be at odds with the factor of only a 100 measured for the difference in the affinity of $tRNA^{Phe}$ compared to $tRNA^{Leu}$ (92). It also opened up the possibility of differences due to the binding environment in the ribosome versus that in the group I intron.

To investigate this issue in the context of the ribosome, the binding of cognate ASL^{Phe}, near-cognate ASL^{Leu} and near-cognate ASL^{Ser} to the 30S subunit with a UUU codon was studied by crystallography, and the affinity of the ASLs for the ribosome were determined in solution, in each case in the presence and absence of paromomycin (132). Measurements were also done with the synonymous cognate codon UUC to determine the affinity differences between C·G and U·G base pairs, both of which are allowed at the wobble position.

The near-cognate ASL^{Leu} and ASL^{Ser} bind to phenylalanine codons with U·G mismatches at the first and second positions of the codon-anticodon helix,

respectively. In each case, clear density for ASL and codon was observed only in the presence of paromomycin. The overall structure of the 30S subunit was then similar to that of the cognate case, but locally there were significant differences as a result of the mismatch. For the ASL^{Leu} the U·G mismatch results in a displacement of the U nucleotide so that contacts between A1493 and the codon are broken (Figure 2*d*). However, there is an additional hydrogen bond that is possible between the N2 of the guanine and the N3 of the adenine, so that there is a net deficit of one hydrogen bond. A single hydrogen bond causes only an additional stabilization of about 2–6 kJ/mol in an aqueous environment because the free energy gained during their formation and the liberation of free solvent only barely compensates for the loss of the hydrogen bonds of the free, individual interaction partners with water (41). However, in the interaction of A1493 with the minor groove of the U·G pair, certain hydrogen bonds are no longer made, but the bonding partners are left desolvated because they are not accessible to water. This leaves unsatisfied hydrogen bonding potential at the 2′ OH groups of the codon uridine and A1493. Therefore, compared to the cognate base triple, this near-cognate interaction will be destabilized by roughly the cost of desolvation. In a study of a series of inhibitors of the protease thermolysin, an analogous situation led to a loss in affinity of around three orders of magnitude (around 17 kJ/mol in terms of binding energy $\Delta\Delta G$, at 37°C), compared to fully-hydrogen-bonded ligands (133, 134).

In the second position, the density observed for the U·G base pair was most consistent with Watson-Crick rather than wobble geometry (Figure 2*e*). Although alternative explanations were also proposed (132), the most straightforward explanation is that either the U or the G has undergone tautomerization to the enol form, thus allowing pairing with Watson-Crick geometry. Thus the ribosome in the presence of paromomycin may accommodate mismatches in either of two distinct ways: With a U·G mismatch at the first position, it retains the normal tautomer and wobble geometry of the base pair, but pays the energetic penalty, owing to desolvation and loss of interactions. At the second position, it appears more favorable for the ribosome to retain the interactions at the minor groove but stabilize an unfavorable base tautomer. These are probably not fixed rules that apply to the first and second codon positions, but rather, the situations that arise may vary with other mismatches (e.g., A:C or C:A). Both of these imply a difference in binding energy of 15–20 kJ/mol or an affinity ratio of 10^{-3}–10^{-4} between cognate and near-cognate tRNA.

How well do the relative affinities suggested by these structures agree with actual binding affinities measured for tRNA-ASLs in solution? At the wobble position, the difference in affinity between a C·G and U·G pair (obtained by comparing a UUC codon with a UUU codon with the cognate ASL) is a factor of ∼10 (132), consistent with the conclusion from the structure that the ribosome does not monitor the geometry of base pairing at the wobble position. In contrast, at the first two positions, in the presence of paromomycin and a UUC codon, the affinity difference between a U·A pair and a U·G mismatch is roughly 1500–3000, corresponding to a $\Delta\Delta G$ of 15–20 kJ/mol. This suggests that the ribosome

does indeed discriminate strongly at the first two positions between cognate base pairs and mismatches. Paromomycin increased the affinity of cognate ASL by approximately a factor of 15 but, rather surprisingly, did not measurably change the affinity of near-cognate tRNA (132). This observation stood in contrast to the expectation that paromomycin would increase the stability of near-cognate tRNA. However, it is in fact consistent with the conclusion that paromomycin primarily affects an induced fit rearrangement of the ribosome during decoding, a conclusion that had previously also been drawn in general terms from kinetic data (107).

Indeed, the 30S crystal structures showed that, in the absence of paromomycin, near-cognate ASL does not induce the domain closure seen on binding cognate ASL. Together with the unchanged affinity for near-cognate ASL with and without paromomycin, this suggested that the absence of visible density for the ASL in the structures was due to its being disordered in an open A site rather than lack of binding. However, the presence of paromomycin allows domain closure even with near-cognate ASL.

Given the role of paromomycin in increasing incorporation from near-cognate tRNAs, it was concluded that the domain closure observed in the 30S crystal structure was an essential feature of tRNA selection (132). In order for this domain closure to be energetically favorable on the timescale relevant to tRNA selection, its cost must be paid for by the additional interactions the ribosome makes only with cognate codon-anticodon pairs in the closed form of the 30S (see below). In particular, the interactions of G530, A1492, and A1493 with the codon-anticodon helix minor groove make the transition to the closed form favorable for cognate but not near-cognate tRNA.

Cryo-Electron Microscopy Structures of the Ribosome

In the past decade, single-particle reconstruction on images from cryo-electron microscopy (cryo-EM) has provided structures of the ribosome of increasing resolution (135, 136). Because the quantities of material required are extremely small and there is no need for crystals, the technique is particularly suited for studying ribosomes trapped in various functional states. Whereas initially the resolution was limited to 20–30 Å, it is now not uncommon to see structures of the 70S with resolutions better than 10 Å, with prospects of further improvement. Quite apart from improvements in resolution, cryo-EM on the ribosome has recently become even more powerful: Because crystallography on the ribosomal subunits has resulted in atomic models for each, it is now possible, to a certain degree, to interpret the low- or medium-resolution maps from cryo-EM in molecular terms.

In connection with the problem of decoding, the structure of the ternary complex of EF-Tu, tRNA, and GTP bound to the ribosome with a cognate codon in the A site has been of particular interest. Although this complex is not accessible to structural studies because of its transient nature, the complex of tRNA and EF-Tu with GDP and kirromycin bound to the A site of the ribosome is quite stable.

Moreover, at the resolution of the cryo-EM structures, it probably represents something close to the GTPase-activated form because kirromycin prevents the transition of EF-Tu from the GTP to the GDP form (137, 138). It has been questioned whether the kirromycin-stalled complex is on the translation pathway (139). However, this objection ignores kinetic data showing that, in the presence and absence of kirromycin, fluorescent signals from both the proflavin and the mant-dGTP reporters are identical prior to GTP hydrolysis (90). Following GTP hydrolysis, the data are consistent with the idea that kirromycin prevents the conformational change in EF-Tu and the subsequent release of the factor and accommodation of tRNA. Thus, the kirromycin-stalled complex of the ribosome with EF-Tu and tRNA is in fact quite relevant to an understanding of decoding.

The first such complex determined (140) showed that EF-Tu presented tRNA at a significantly different orientation than the fully accommodated A-site tRNA after the acceptor end swung into the peptidyl transferase site. This finding was consistent with previous footprinting experiments, showing that the tRNA complexed with EF-Tu bound in the A site of the 30S but not the 50S subunit (141). By itself, this raised certain questions about the recognition of the codon-anticodon helix elucidated by crystallography on the 30S subunit. In the 30S crystal structures, the conformation of the ASL is close to that of the fully accommodated tRNA. However, it is known from biochemical and kinetic data that codon-anticodon recognition precedes GTP hydrolysis. Therefore, it was not clear how relevant the 30S structures were to initial recognition of codon-anticodon pairing. The fact that the A-site tRNA footprints on the 30S were the same regardless of whether EF-Tu was bound to the ribosome or not (142) suggests that the same minor groove recognition by G530, A1492, and A1493 must occur even before GTP hydrolysis by EF-Tu, but it was not clear how this could happen if the orientation of the tRNA was significantly different. The resolution of this puzzle had to await higher resolution cryo-EM structures of the EF-Tu-ribosome complex.

Recent cryo-EM structures of the kirromycin-stalled complex at 16–17 Å (using the criterion of a 0.5 cutoff in the Fourier shell correlation coefficient) from both the van Heel and Frank groups show much greater detail (Figure 4) (143, 144). Perhaps the most striking finding from these structures is that the tRNA is significantly distorted in the kirromycin-stalled complex relative to the crystal structure of the ternary complex alone (145). There appeared to be some disagreement about the nature of the distortion in the tRNA. The van Heel group suggested that this is mainly a distortion in the anticodon loop (144), which would be consistent with the conformational variability of the loop already known by a comparison of various crystal structures containing tRNA. However, the Frank group suggests that the distortion is higher in the body of tRNA (143), and a more recent structure at even higher resolution suggests that it is between the ASL and the D stem-loop (Figure 4*a*) (146).

Because atomic models of the ribosomal subunits were now available, it was possible to deduce the ribosomal contacts of the ternary complex. In particular, both groups agree that S12 makes contacts somewhere along the acceptor arm

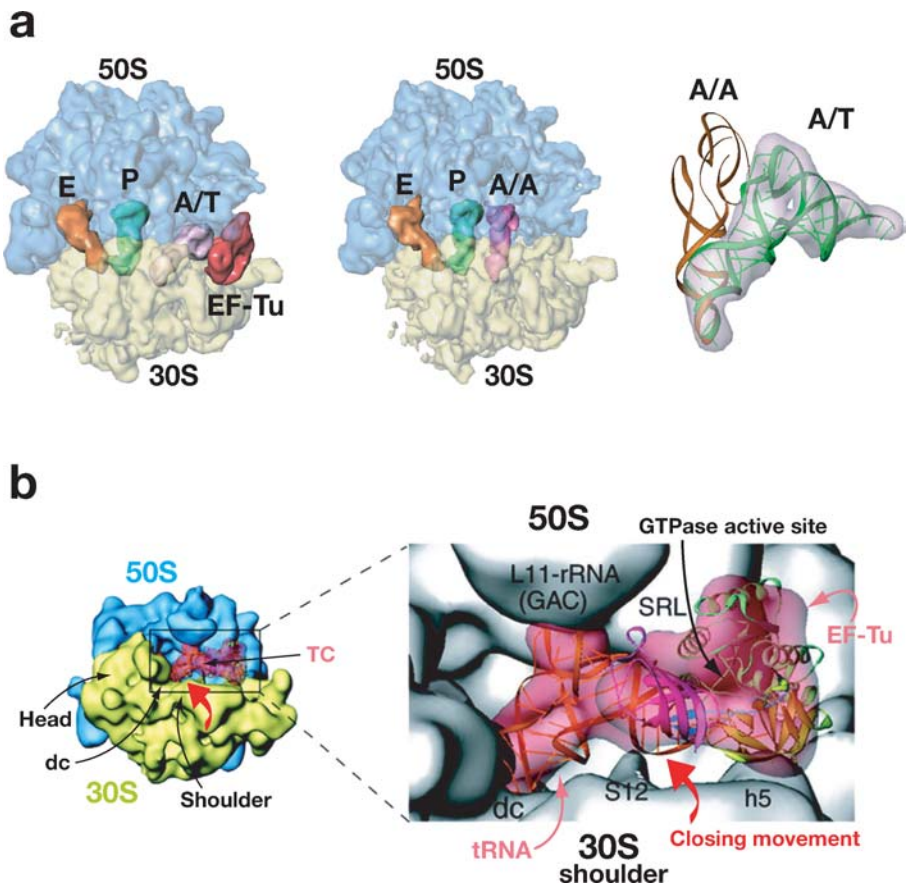

Figure 4 (*a*) Overviews of cryo-EM structures of the ribosome with E- and P-site tRNAs and with ternary complex (*left*) or accommodated A-site tRNA (*center*), and density showing a better fit for bent rather than straight tRNA in the ternary complex bound to the ribosome (*right*). Reproduced with permission from (146). (*b*) Details of the environment of the ternary complex, in the context of the 30S domain closure, indicated by the red arrow. Reproduced with permission from (143). See also the cryo-EM structure of Stark et al. (144).

of tRNA, and that the sarcin-ricin loop (SRL) is close to the nucleotide-binding pocket in EF-Tu (Figure 4*b*). However, the details of the contacts of S12 are not the same in the structures. The L11-RNA region, also referred to as the "GTPase-associated center (GAC)" by the Frank group, appears to make a close contact with the T loop in the elbow region of tRNA in both structures. However, the van Heel group suggests this is an interaction with protein L11 (144), whereas the Frank group suggests that it is close to the region of 23S RNA containing the 1067 loop (143).

AN INTEGRATED MODEL FOR DECODING

Among the long-standing questions concerning the mechanism of decoding were the following:

- How could correct codon-anticodon pairing in the 30S subunit lead to GTP hydrolysis by EF-Tu about 75 Å away?
- Why do many disparate mutations, especially in the 30S subunit (but also in the 50S subunit, EF-Tu, and the tRNA), result in changes in the accuracy?
- Finally, how do antibiotics exert their effects on accuracy?

Crystallography on the 30S subunit, in conjunction with the cryo-EM results and previous kinetic data discussed above, led to an integrated model for decoding that could mechanistically connect events at the decoding center with the selection of tRNA (132, 147). Briefly, the model suggests that the interactions of ribosomal bases with the minor groove of the codon-anticodon helix discriminate on the basis of base-pairing geometry. The binding energy from these interactions is sufficient to induce a domain closure of the 30S subunit for cognate but not near-cognate tRNA. The movements thus induced would also make elements of the 30S shoulder more closely interact with both tRNA and EF-Tu, thus stabilizing a transition state for the ternary complex that involves a distorted tRNA and changes in EF-Tu and the 50S subunit. As discussed below, the model can rationalize a large body of structural, genetic, and biochemical data.

The initial step is binding by the ternary complex to the ribosome. This binding is characterized by a modest increase in proflavin fluorescence. The increase is not due to contacts made with the ribosome because potassium iodide quenches the fluorescence to the same extent in the absence and the presence of the ribosome (148). Rather, it is likely that there is a structural change in the tRNA that changes the local environment of the proflavin reporter in the D loop. What could this change be? It is likely that the initial binding of the ternary complex leads to a deformation of the tRNA because the binding of EF-Tu at this site is incompatible with a straight tRNA, owing to potential clashes with helix 69 and possibly the P-site tRNA. Nevertheless, this initial binding with a possible distortion of tRNA does not represent the transition state because the change in proflavin fluorescence is observed regardless of whether cognate, near-cognate, or even noncognate tRNA binds, indicating that it is independent of (and precedes) codon-anticodon interaction. This stands in contrast to the signal from wybutine at position 37, which monitors the anticodon environment of the tRNA and is not observed with noncognate tRNA.

Almost by definition, the discrimination of correct versus incorrect codon-anticodon base pairing is the key step in decoding. In order to allow codon-anticodon base pairing, the tRNA may need to be distorted even more than during initial binding. This could explain why the codon recognition step is accompanied by a much greater increase in the proflavin signal (89). The most recent

cryo-EM structure suggests a kink somewhere between the ASL and the D stem-loop in a way that would bring the ASL into roughly the orientation it would have after accommodation, while keeping the acceptor end bound to EF-Tu (146). This is consistent with the view that the much larger change in proflavin fluorescence, attributed to codon recognition, could arise from unstacking of the D stem-loop from the ASL of the tRNA. The fact that this increased proflavin signal is seen for cognate and near-cognate tRNA but not for noncognate tRNA suggests that base pairing is required for stabilizing this bent form of tRNA. At this point, the ribosome discriminates between cognate and near-cognate tRNAs by the interactions of the ribosomal bases A1492, A1493, and G530 with the minor groove of the codon-anticodon helix (128). These interactions are favorable for cognate but not near-cognate pairing (132). They discriminate between Watson-Crick and other base pairs at the first two but not the third position of the codon, consistent with the requirements of the genetic code and the wobble hypothesis. The selective stabilization of cognate tRNA, as measured with ASLs on the ribosome in equilibrium measurements (132) as well as from kinetic data (97), is far too high to be accounted for by base pairing between codon and anticodon alone (37–39).

However, this selective stabilization of cognate tRNA is not as high as one might expect from the minor groove interactions. This is because part of the additional binding energy from the minor groove interactions is used to induce a domain closure in the 30S subunit (132). This domain closure does not normally occur for near-cognate tRNA. We believe that this domain closure is the start of a process that transmits the signal of codon recognition to the 50S subunit and eventually leads to GTP hydrolysis by EF-Tu. In the 30S crystals, both the head and shoulder domains move significantly upon occupation of the A site by cognate codon and ASL. However, it is the shoulder movement that appears to be directly relevant to the tRNA selection mechanism. The wealth of genetic data on modulation of fidelity relates to the movement of the shoulder rather than the head (132, 147). Furthermore, the EF-Tu ternary complex (146) is in direct contact with—and may thus be directly influenced by—the shoulder rather than the head. Indeed, comparison with low-resolution structures of the 70S ribosome (123, 149) suggests that the head is in a rather "closed" position, inclined toward the 50S subunit, even in the absence of tRNA, but no comparison was done to a ribosome with tRNA bound in the A site. Definitive evidence for a movement of the head during decoding, if any, must come from high-resolution structures of the 70S ribosome with and without A-site tRNA.

The primary transmission appears to be via protein S12 and helix 15 in the shoulder domain of the 30S subunit. In the domain closure, protein S12 would interact more closely with the acceptor arm of tRNA in the ternary complex, and helix 15 would similarly make closer contacts with EF-Tu. Thus, domain closure in the 30S results in a transmission of the signal from the 30S, where codon recognition occurs, to the 50S subunit, partly via tRNA and EF-Tu. These conformational changes, involving domain closure in the 30S subunit and the

accompanying (or concerted) changes in the 50S subunit, tRNA, and EF-Tu, must correspond to the GTPase-activation step that is known to follow codon recognition in the kinetic scheme (90, 91). The result would thus be a conformation of the ribosome that would stabilize the transition state for GTP hydrolysis. Among other things, the transition state is characterized by a distortion in the tRNA (143, 144, 146), as well as a change in the conformation of the GAC, and possibly a movement of the tRNA acceptor end relative to EF-Tu (146). Because the minor groove interactions and the resulting domain closure are not favorable for near-cognate tRNA owing to the large energetic penalties involved (132), the GTPase-activation step is much slower for near-cognate tRNA (92).

After GTP hydrolysis and release of EF-Tu, the distorted tRNA conformation is energetically highly unfavorable. However, while the tRNA relaxes into its most favorable, straight-armed conformation, the ASL is constrained by the closed form of the 30S subunit in roughly the accommodated orientation (132). The fixed position of the ASL means that a greatly reduced conformational space is accessible to the remainder of the tRNA during its relaxation and that this relaxation will result in the accommodated state, thus speeding up the process. This explains why it is not merely the dissociation rate of tRNA that is lower for cognate tRNA, but the forward rate of accommodation should also be accelerated (92).

The 30S domain closure model, described above, places the code at the conceptual center and describes decoding as the transmission of a signal from codon-anticodon recognition through the 30S to the entire ribosome-tRNA-EF-Tu complex, resulting in GTP hydrolysis and accommodation. Subsequently, Valle et al. proposed a related but more 50S-centric model for decoding (146). Because of the observation that the L11 region (or GAC) of the 50S subunit is in a more compact or "closed" conformation in the ribosome with a kirromycin-stalled ternary complex, it was proposed that this closed-GAC form of the ribosome represents an activated state that induces a greater flexibility in the tRNA, and this form would facilitate codon-anticodon interactions. Stabilization of this closed form by codon-anticodon interactions in the 30S subunit would then lead to GTP hydrolysis by EF-Tu. However, the cryo-EM structure represents a state reached after GTP hydrolysis, so it is not currently clear whether the closed conformation of the L11 region is reached immediately upon ternary complex binding. But even if that were the case, binding of ternary complex to the ribosome could not immediately result in an active state for GTP hydrolysis that merely has to be stabilized by codon-anticodon recognition. This is because kinetic data show that initial binding, codon recognition, and GTPase activation are distinct and sequential steps (90). As stated above, the codon-recognition step is likely to involve distorted tRNA for both cognate and near-cognate tRNA, as judged by the proflavin fluorescence. However, kinetic data also show that something else after stabilization of codon recognition has to happen that accelerates GTPase activation for cognate but not near-cognate tRNA. This is easier to explain with the 30S domain closure model discussed earlier, proposed on the basis of crystallography and affinity measurements on the 30S subunit.

Following GTP hydrolysis, Valle et al. (146) propose that the tRNA acts like a molecular spring and is accommodated rapidly. This is essentially the same notion as the idea that "tRNA can relax from a strained conformation into the accommodated state," proposed above in the context of the 30S domain closure model (132). However, the 30S domain closure model also suggests how the constraints imposed on cognate ASL can affect the forward rate of accommodation (as opposed to just the dissociation rate) for cognate relative to near-cognate tRNA by restricting the conformational space available to cognate tRNA during accommodation. Finally, in evolutionary terms, one can imagine that the 30S domain closure could occur even in a primordial all-RNA ribosome since it depends on interactions of tRNA with the RNA component of the 30S subunit. Factor-free translation has been demonstrated even in today's ribosomes (150). Thus, induced fit of the 16S RNA to the codon-anticodon minor groove could be an ancient feature of decoding. An open decoding site in the ribosomal RNA allows rapid screening of all the different tRNAs against a certain codon. The closed conformation of the decoding center in the 30S subunit then confers high specificity of codon-anticodon pairing and also accelerates accommodation of the tRNA aminoacyl end into a position in which it takes part in peptide bond formation. EF-Tu and the activation of its GTPase activity by codon-dependent induced conformational changes in the ribosome are, most probably, a later addition to enhance speed while further improving accuracy.

Stark et al. (144) do recognize a probable involvement of the decoding-site 16S RNA contacts with the codon-anticodon duplex in the deformation of tRNA, which they independently observed, and also in GTPase activation. These authors also favor a model whereby GTPase activation is mediated via the acceptor end of tRNA and the SRL. However, because the movement of the 30S shoulder is missing from that model, it provided a less straightforward explanation of why the tRNA and SRL assume these roles in a codon-dependent way.

An unrelated theoretical model of decoding, the transorientation hypothesis, was published recently (139). This model relies on a proposed switch of the anticodon from a 3′ to a 5′ stack, similar to an earlier proposal for such a switch during translocation (151). The model has very little support from the experimental data. Despite the many crystal structures containing tRNA in various contexts, a 5′ stack has yet to be observed. It has also been criticized on the grounds that it would be incompatible with the 70S structure (152).

RELATIONSHIP TO PRIOR GENETIC AND BIOCHEMICAL DATA

The recent insights into the mechanism of decoding discussed above finally make it possible to understand in structural terms a large body of biochemical and genetic data accumulated over the past four decades. Some of these are discussed below.

Paramomycin

The crystal structures show that paromomycin displaces A1492 and A1493 entirely out of the internal loop of helix 44 into a position where they could make contact with the minor groove of the codon-anticodon helix (124, 128). On a more global scale, the binding of paromomycin alone also induces a partial closing movement of the whole 30S shoulder, in particular protein of S12 toward helix 44 of the 16S RNA (128, 147). Thus, paromomycin induces part of the conformational change that is seen on tRNA binding to the A site. Kinetically, however, a major effect of paromomycin is to increase the forward rates of GTPase activation and accommodation of near-cognate tRNA to the point where they are comparable to that of cognate tRNA (107). In equilibrium measurements with cognate ASL on the ribosome, it was also shown that paromomycin increases the stability of cognate tRNA by a factor of 15 but has little effect on the stability of near-cognate tRNA.

These data are consistent with the idea that paromomycin pays for part of the energetic cost of domain closure that is induced by cognate tRNA. In the case of cognate tRNA, the ribosome reaches the closed state regardless of whether paromomycin is present or not, thus leading to an increase in affinity. Near-cognate tRNA, however, cannot induce domain closure in the absence of paromomycin but can do so in its presence. Thus, affinity measurements of cognate versus near-cognate tRNA compare the closed form in the cognate case (with its associated cost of induced changes) with the open form in the near-cognate case (without such costs), leading to an underestimate by a factor of about 15 in the intrinsic selectivity. These ideas make perfect sense in terms of the kinetic data: The domain closure leads to, or is coupled with, GTPase activation, and by making domain closure favorable, paromomycin increases the rate of GTPase activation. Other aminoglycosides that act like paromomycin, e.g., neomycin, gentamycin, or kanamycin, are expected to have similar underlying mechanisms.

Streptomycin and *ram* and Restrictive Mutants

Streptomycin (Sm), the first antibiotic known to target the ribosome, has long been a puzzle. Although it was clear early on that it increases the error rate of protein synthesis (22), its mechanism has been far from clear. Studies of accuracy in vitro suggest that streptomycin affects both initial selection and proofreading (83, 153, 154). The best evidence for the action of streptomycin comes from recent kinetic studies. These studies show that streptomycin lowers the forward rates of GTPase activation and accommodation for cognate tRNA but increases them for near-cognate tRNA (155, 156).

A structural explanation for these observations has been proposed (147). The structure of the 30S subunit with streptomycin (124) suggests that streptomycin stabilizes a variant of the closed form. However, it appears that the way streptomycin achieves this would prevent the 30S shoulder from moving as far in the direction of the 50S subunit and EF-Tu as is observed when a cognate codon-anticodon

duplex is recognized. This suggests that streptomycin promotes a suboptimal state for GTP hydrolysis. This suboptimal state would result in a GTPase-activation rate that is lower than normal for cognate tRNA but that could be reached even with near-cognate tRNA.

The recent crystal structures show that mutations in the 30S subunit that affect accuracy are distributed over a large region; many of them are quite far from the codon-anticodon helix (124, 147). Two particular classes of mutations are the *ram* mutants that lower accuracy and the *str* mutations that confer streptomycin resistance and increase accuracy.

Many of the *ram* mutations would disrupt the interface between proteins S4 and S5. This interface contains a number of salt bridges in the open form of the 30S subunit. During domain closure, this interface is disrupted with the two proteins moving apart slightly (Figure 3) (132). The breaking of bonds at the S4-S5 interface would thus contribute to the energetic cost of domain closure. If the interface were already disrupted owing to mutations, this energetic cost would be lowered and would result in a higher probability that near-cognate tRNA could also induce domain closure, leading to tRNA selection and thus lowering accuracy.

Restrictive mutants have the opposite effect. An examination of the structures shows that additional contacts are made between S12 and ribosomal RNA in the closed form, thus leading to its stabilization (Figure 3). Mutations that disrupt these additional contacts would result in a destabilization of the closed form and also an increase in the energy barrier to its formation, leading to an increase in accuracy, although at the expense of speed. Thus, these mutations, which confer streptomycin resistance, offset the effect of streptomycin rather than prevent its binding.

A Role for the Structural Properties of tRNA

A role for the properties of tRNA in the decoding mechanism has long been advocated by many on the basis of mutations in tRNA distant from the anticodon loop (Figure 5) (e.g., References 57, 89, 157, and 158). In the first such mutant to be identified, the Hirsh suppressor, a G24A mutation within the D arm of Trp-tRNA^{Trp}, could promote Trp incorporation on UGA stop codons (69, 70). It was shown that this mutation was correlated with a decrease in the rate of UV-induced cross-linking between tRNA residues 8 and 13 (159), which are located on the inside of the tRNA "elbow," not far from the G24A mutation (Figure 5). Conversely, the 8–13 UV cross-link decreased the frequency of UGA misreading by the Hirsh suppressor (160).

Nucleotides 9, 12, and 23 of tRNA form a base triple in the D stem of the anticodon arm and are located between the Hirsh G24A mutation and the 8–13 cross-link (Figure 5). Smith & Yarus (161, 162) found that the disruption of this base triple by the A9C mutation has the same error-inducing effect (allowing a normally forbidden codon-anticodon A3:C34 wobble) as the Hirsh mutation. By mutational analysis of both the 24:11 base pair and the 9:12:23 base triple, they concluded that

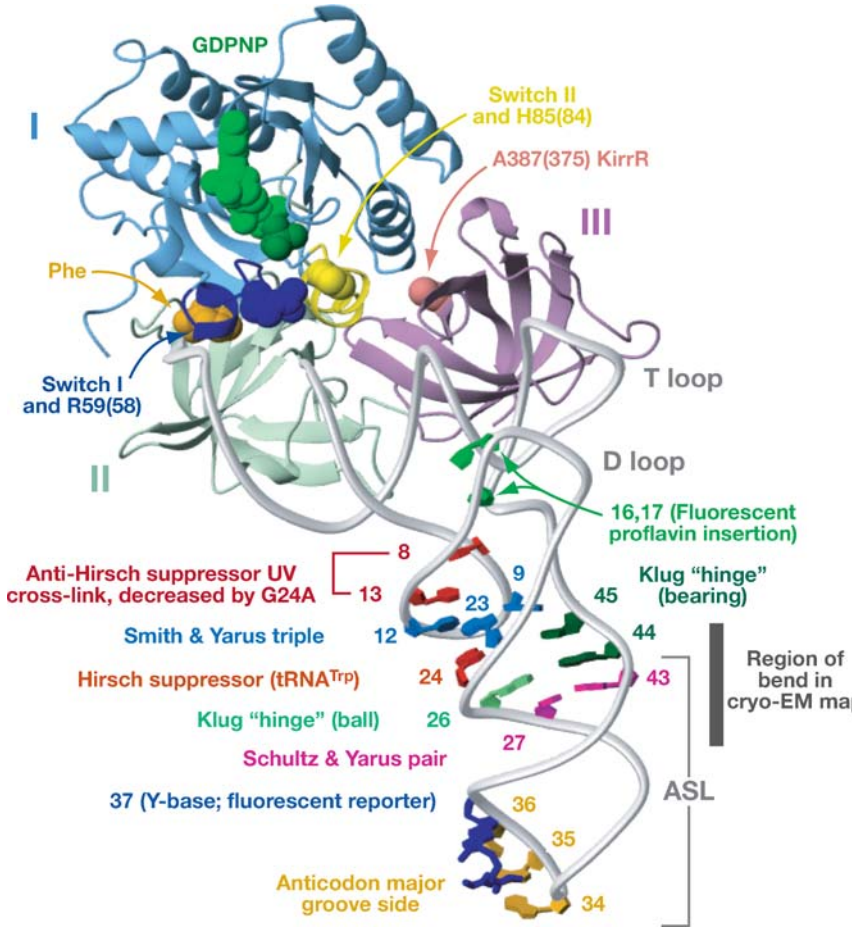

Figure 5 Structure of the ternary complex of EF-Tu, tRNA, and a GTP analog (208). Elements of tRNA and EF-Tu that are known or likely to be involved in translational fidelity or that were used as reporters have been mapped onto the structure.

misreading is increased when either the 9:12:23 triple is disrupted directly (by A9C mutation) or its disruption is favored by the introduction of a potential, alternative tertiary interaction of A9 with position 24, which is not observed in the crystal structure, owing to the mutations G24A or G24C (161, 162). Similarly, at the top of the tRNA anticodon stem, three bases 3′ to the Hirsh mutation, disruption by site-directed mutagenesis of the Watson-Crick base pair 27:43 (Figure 5) has the same error-prone phenotype as the G24A or A9C perturbation of D stem structure (163, 164).

The domain closure in the 30S subunit, induced by cognate but not near-cognate tRNA binding (132, 147), and the resulting stabilization of a distorted tRNA

observed in cryo-EM structures (143, 144, 146) make it possible to rationalize these data. Thus, tRNA tertiary structure around and below the elbow is perturbed, or "strained," during normal tRNA selection, so that only the additional binding energy from discriminating interactions at the cognate codon-anticodon helix are sufficient to stabilize the distorted tRNA in the transition state. However, if mutations render this region of the tRNA more easily deformable, then a similar stabilization could occur with increased probability even if the interactions in the decoding center are near cognate (132, 147). A similar point was made by Yarus et al. (165) when they revisited the tRNA mutational data in light of the cryo-EM structures; they concluded that tRNA deformation "sets a threshold for biologically acceptable decoding." The requirement of a strained and distorted tRNA during tRNA selection also makes it possible to rationalize the observation that GTP hydrolysis does not occur with fragmented tRNA (166).

Flexibility of the tRNA within the anticodon arm was originally postulated on the basis of the tRNA architecture alone. In their analysis of the original yeast $tRNA^{Phe}$ structure, Klug and coworkers noted a possible hinge between the D stem and the anticodon stems of the anticodon arm, where unpaired base 26 would lie "in the bearing formed by 44 and 45" (167), see Figure 5. Both this 44–45 hinge and the 27:43 base pair discussed above (163, 164) are located intriguingly close to the "kink" in the tRNA anticodon arm visualized in the cryo-EM map of the kirromycin-stalled ternary complex of Frank and coworkers (143, 146).

All of this suggests that the deformation in the tRNA need not be constrained to one defined point. Indeed, the distribution of the conformational effects of codon-anticodon recognition throughout the tRNA is expected: The directionally opposing forces originating from the 16S RNA-codon-anticodon interaction at one end, and from EF-Tu at the other end, of the tRNA are separated by more than 70 Å. A further important point of contact, the L11-RNA region, lies about midway between the two ends of the tRNA and is likely to have an important role in stabilizing the distortion (143, 144, 146).

Interactions with EF-Tu and the 50S Subunit

An important, currently unresolved issue is the composition and structure of the EF-Tu GTPase active site. Although there is no indication that the ribosome directly inserts a catalytic residue, there are also no convincing candidates in EF-Tu itself, as judged by crystal structures and mutational studies (168, 169). It is also known that kirromycin and the closely related aurodox somewhat stimulate the GTPase activity of EF-Tu even in the absence of the ribosome (170). On this basis, the crystal structure of EF-Tu:GDP bound to aurodox suggests that a particular histidine residue (His84) might contribute to transition state stabilization during GTP hydrolysis (138). The cryo-EM models of ribosome-bound ternary complex place both His84 and the GTP-binding site of EF-Tu close to the SRL (143, 144).

The SRL is known to play a central part in translation. Either depurination of A2660 or cutting the SRL between G2661 and A2662 by the protein toxins ricin or α-sarcin, respectively, abolishes translation by hindering proper association of EF-Tu and EF-G (reviewed in 86) (the equivalent applies in eukaryotic translation). This emphasizes the importance of the direct contact to EF-Tu close to the GTP-binding pocket. The mutation G2661C in the SRL (171) reduces the association and GTPase rate of the ternary complex and leads to translational hyperaccuracy (172). This mutation would thus be expected to compromise the interactions that induce the active conformation of the EF-Tu GTP-binding/GTPase site. In the additional presence of a restrictive mutation in S12, the ternary complex association rate is further reduced, and the overall stringency of in vitro translation increased. This double mutation is lethal unless streptomycin is included in the medium, in which case the hyperaccuracy also decreases to a level of accuracy well below wild type (172). Such a phenotypic relation is expected if there is direct conformational coupling between the 30S shoulder, EF-Tu, and the SRL. If mutations render the closure of the 30S shoulder into an active conformation more energetically demanding, in addition to compromising interactions at the SRL, too much functionality is lost unless the closed conformation of the shoulder is supported by Sm.

Further, the G2661C/S12-SmP double mutant can be rescued not only by Sm-mediated reinforcement at the shoulder, but also by certain kirromycin-resistant (KirrR) mutants of EF-Tu (173). These KirrR mutations of EF-Tu alone (Figure 5) cause an error-prone phenotype. It is tempting to speculate that this might be another case in which one set of mutations that increases the energetic demand on conformational changes (S12, SRL–G2661C) is compensated by a mutation that facilitates the same, or equivalent, rearrangements. Kirromycin binds EF-Tu at the interface between domains I and III (Figure 5), which rearrange significantly in the transition to the GDP form of the protein. This domain probably also rearranges somewhat in the transition from the GTP-binding to the active GTPase form (138, 143, 144, 146). The rationalization of the link between error-prone translation and kirromycin resistance is not immediately evident. However, many KirrR mutations are located around this domain I/III interface and could thus indirectly affect the ease of activating the GTP-binding site on the ribosome, again owing to the balanced energetics of concerted conformational changes.

A role of L7/L12 has long been suggested in interaction with translational factors. In a recent study, it was shown that mutations both in L7/L12 and in a certain region of EF-Tu (helix D in domain I) decreased the rate of A-site binding of EF-Tu, primarily because of a decrease in association rate (174). It is not easy to see how this interaction could occur from the cryo-EM structures of the kirromycin-stalled complex (143, 144, 146), suggesting that it may occur at an earlier stage, such as initial binding, or that L7/L12 transiently undergoes a rather dramatic change in conformation. This indicates that much remains to be understood about the precise sequence of events and interactions that occur on ternary complex binding to the ribosome.

DNA as a Template for Translation

It has long been known that DNA is a poor template for translation, but its efficiency can be increased significantly by the antibiotic neomycin, which is very similar to parmomycin (175). It was also shown much later that the presence of a deoxycodon abolishes tRNA binding in the A but not the P site (176). These long-standing observations can now be easily rationalized. The minor groove recognition of the codon-anticodon helix is required for decoding and is a characteristic of the A site. Such recognition is not a characteristic of the P site, where a high level of discrimination is no longer required because the ribosome is already committed to the tRNA at that stage. The minor groove recognition depends on the formation of bonds with the 2′ OH groups of the nucleotides at all three positions of the codon. Thus, these interactions would no longer be favorable for deoxyribose codons and would not lead to domain closure in the 30S and tRNA selection. However, as with near-cognate tRNA, the presence of an antibiotic could allow domain closure even in with deoxyribose codons.

A Common Mechanism Underlying Initial Selection and Proofreading

The kinetic proofreading scheme conceptually separates tRNA selection into initial selection and proofreading steps. Indeed, they are required to be kinetically distinct steps for the scheme to lead to enhanced accuracy. Nevertheless, recent kinetic data suggest that these two steps may share a common underlying mechanism.

Kinetic data show that the forward rates of GTPase activation and accommodation are both accelerated by cognate relative to near-cognate tRNA. Similarly, paromomycin also accelerates both of these rates for near-cognate tRNA (92). Because the rates of near-cognate tRNA were already at the detection limit of the technique, it was not possible to see if paromomycin had any effect on cognate tRNA. Finally, it has recently been shown that streptomycin also affects both forward rates, both for cognate tRNA, where the rates are reduced, and for near-cognate tRNA, where the rates are increased (156). The fact that three quite separate factors (codon-anticodon pairing, paromomycin, and streptomycin) can each affect both of the forward rates suggests that, although kinetically distinct, GTPase activation and accommodation have a common underlying mechanism.

It was pointed out that the underlying mechanism could be the domain closure in the 30S subunit, induced by cognate tRNA binding or by near-cognate tRNA in the presence of paromomycin or streptomycin (132, 147), as outlined above. In the first instance, this domain closure leads to GTPase activation, explaining the acceleration of that step. However, after GTP hydrolysis, as discussed above, the domain closure constrains the ASL of the distorted tRNA in the accommodated orientation, thus speeding up the relaxation of the acceptor end of the tRNA into the peptidyl transferase site by limiting its conformational space.

An interesting question is whether there are specific agents that would preferentially affect one step or the other step. It has been proposed that tetracycline, which binds in the A site but allows GTP hydrolysis by EF-Tu, would not allow

accommodation (177). Another interesting possibility is that the Hirsh suppressor tRNA may work by being more easily distortable, as proposed above. It is likely to speed up GTPase activation but may not necessarily be faster in accommodation. Agents that affect the two steps in different ways are likely to shed light on the underlying mechanisms.

A Role for E-Site tRNA in Fidelity

It has been suggested that the A and E sites of tRNA are negatively coupled allosterically, and the presence of E-site tRNA reduces the affinity of ternary complex for the A site and increases accuracy (178). It is possible to speculate that the induced conformational changes, discussed above, would have a higher energetic penalty if the E site were occupied, perhaps because of interactions that E-site tRNA would make with elements of the head, e.g., S7, that would have to be broken. However, as originally proposed, the low affinity was a barrier to noncognate rather than near-cognate tRNA. In the detailed model proposed above, the induced conformational changes differ between cognate and near-cognate tRNA. Thus, the exact details of what role the E-site tRNA plays in fidelity will have to await both structural and kinetic work that compares ribosomes with an empty versus an occupied E site.

The Helix 27 Switch

Helix 27 is a highly conserved stem-loop of 16S RNA that is packed closely against helix 44 near the decoding site. Different mutations in helix 27 both increased and decreased the accuracy of translation (179). Earlier examination of the sequence of helix 27 had suggested that there were two alternative base-pairing possibilities (180). This led to the notion that helix 27 was a conformational switch that effected a transition from a *ram* to a restrictive state of the ribosome.

Although this was an attractive idea, several problems began to emerge with the model. The first was that the accuracy phenotypes could not be reproduced in a eukaryotic system, even though the sequence of helix 27 is highly conserved (181). The structure of the 30S subunit (118) suggested that this helix was tightly packed, and it was difficult to see how it could change its internal base pairing without extensive disruption of the neighboring region. Finally, a high-resolution structure of a streptomycin-dependent 30S subunit (182) as well as a low-resolution structure of a similar 70S ribosome (149) showed no change in the conformation of helix 27 compared to the wild type.

Recently, the helix 27 switch model was revisited by the laboratory that originally proposed it (183). They constructed a helix 27 with quadruple mutations that would severely disrupt its proposed alternative conformation without affecting the conformation observed in the various crystal structures. This mutant ribosome was normal in its function, thus suggesting that the switch did not occur during translation. Therefore, although the helix 27 switch model certainly led many workers to think about conformational changes in ribosomal RNA, it must no longer be considered a realistic possibility in the translation process.

Modified Bases in tRNA

The general principles of decoding depend on Watson-Crick base-pairing interactions. However, there are particular tRNA-codon combinations in which this alone, even with minor groove recognition, is insufficient to facilitate decoding or even stable binding of tRNA to the A site. Indeed, only 7 of the 61 codons in *E. coli* are read exclusively by a tRNA without modifications at position 34 or 37 (184, 185). A striking example of the importance of modifications is lysine tRNA, which has modifications at positions 37 and 34. Without the former, it cannot bind stably to either lysine codon. The single modification at position 37 facilitates binding to the AAA codon, although both are required to also bind the AAG codon (186, 187). Entropic contributions by preordering of the anticodon loop (186) have been inferred from NMR structures of a modified ASL. Kinetic data show that stacking interactions of the tricyclic base wybutine make a large energetic contribution to the free energy of the codon-anticodon interaction on the ribosome (188). Both of these suggest a balance between the energy gained from tRNA binding and the energy required to reach a productive form for tRNA selection. It is clear that modifications fine-tune this balance, and in many cases are absolutely required for function. Recent crystal structures of the appropriately modified lysine ASLs to 30S subunits with AAA and AAG codons in the A site provide support for the notion that stacking and entropic contributions are likely to make decoding favorable for the appropriately modified ASL and not for the unmodified one (188a).

Relationship to Frameshifts

Errors in decoding would generally give rise to missense errors that often lead to conservative substitutions, which would not affect protein function significantly. Frameshifts by the ribosome would usually be far more deleterious to the cell because they generally result in a truncated protein. Are frameshifts related to decoding? Early observations showed that the level of frameshifting was reduced in restrictive mutants but increased in *ram* mutants or by streptomycin (189). This almost perfect correspondence with errors in decoding suggests a connection between the two. One mechanism suggested for +1 frameshifts is a four-base interaction between codon and anticodon (e.g., References 190 and 191). However, recent work suggests that frameshifts may be controlled by interactions at the P site, reviewed in References 192 and 193. Recently a role has also been proposed for codon-anticodon interactions in the E site to maintain a reading frame (194). Structures of the ribosome in appropriate contexts will go a long way toward clarifying the mechanisms underlying frameshifting and other unusual properties of the ribosome.

Similarity to Other Polymerases

It has often been said that if the ribosome had been discovered by biochemists rather than cell biologists, it might well have been called "polypeptide polymerase." Like

DNA and RNA polymerases, it uses a nucleic acid template and base complementarity to direct synthesis of a polymeric product. Interestingly, it shares a number of similarities with DNA and RNA polymerases.

It has previously been pointed out that DNA polymerases, like the ribosome, also undergo an induced fit upon binding of the correct incoming nucleotide, and this results in an acceleration of forward rates (36). The structural work shows that this analogy extends much deeper. All known crystal structures of DNA and RNA polymerases have conserved amino acids that interact closely with the minor groove of the critical base pair between the template and transcript strands (e.g., References 195–197). These interactions would be sensitive to the shape of the base pair, just as the interactions of the 30S ribosomal subunit with the codon-anticodon helix are at the first two positions. An interesting exception is that highly error-prone DNA polymerases involved in lesion repair do not have this minor groove recognition (198).

Interestingly, a series of experiments have shown that DNA polymerase will accept base pairs that have the right shape even if they do not have any hydrogen-bonding interactions at their Watson-Crick interfaces (199, 200). Finally, polymerases also use part of the free energy from the binding of the correct substrate to induce a transition to a closed, productive form (201–203).

CONCLUSIONS

Many of the ideas that have emerged from structural work so far need to be tested biochemically. Additional reporters for presteady-state single-turnover kinetics, for example at the S4-S5 interface, elsewhere on the tRNA, or on the 50S subunit, as well as data from mutant ribosomes, will greatly help to clarify the nature of the processes involved. Moreover, a recent paper shows that single-molecule experiments have the capacity to further dissect various kinetic steps and may play an increasingly important role in the future (203a). Finally, although many of the states may eventually be well-characterized, an understanding of the transitions between states may not emerge from experimental work alone and may require other methods, such as molecular dynamics. Some initial work in this area has already begun (204).

A number of important mechanistic issues remain. We need to understand the details of the distortion in tRNA during the initial selection process. It is possible that the flexibility of different tRNAs are carefully calibrated to compensate for the strength of the interactions at the decoding center, in the same way that the affinity of tRNAs for EF-Tu is calibrated to compensate for differences in the affinity of the various amino acids for the factor (205). A major issue in the field is to understand the detailed interactions of translational factors with the ribosome and, in particular, the mechanism by which the ribosome activates the GTPase activity of factors. These questions will require high-resolution structures of the ribosome and the ternary complex in various states, preferably with different tRNAs for

comparison. The mechanism by which stop codons are recognized and decoded by release factors needs to be understood in structural terms.

Nevertheless, the work of the past few years, discussed in this review, has qualitatively changed our understanding of the mechanisms underlying translational fidelity. Base complementarity is a fundamental principle in replication, transcription, and protein synthesis, but the property of base complementarity that gives rise to selectivity has been a matter of debate. In translation, this debate has often been posed in apparently conflicting terms, such as geometric recognition of Watson-Crick base pairs versus kinetic enhancement of fidelity.

It is clear that the ribosome does discriminate between the geometry of cognate and near-cognate base pairs. It does not do so at the wobble position, which provides an explanation for the long-standing puzzle of why Watson-Crick pairs are required at the first two positions of the codon but not the third. However, the level of geometric discrimination alone would result in an affinity ratio comparable to the fidelity of translation. Why was this level of stabilization not seen on the ribosome?

It now appears that cognate but not near-cognate ASL induces a transition to a closed form of the 30S subunit. However, in the presence of paromomycin, both near-cognate and cognate ASL could induce the transition to the closed form. Thus, stability measurements made in the absence of paromomycin compare two different states of the ribosome, the closed form for cognate versus the open form for near-cognate. Because reaching the closed form requires an energetic cost, the affinity of cognate tRNA is lowered, resulting in an apparently lower stabilization of cognate tRNA. What benefit could a loss of stability confer?

The maximum possible binding affinity is sacrificed by using part of the binding energy to pay for the cost of a transition to a closed form. However, this movement allows it to reach the transition state for GTP hydrolysis by EF-Tu, which involves a distorted tRNA. After GTP hydrolysis, it also accelerates the forward rate of accommodation. Although the greatest possible accuracy is compromised, these rate accelerations ensure that the ribosome is able to quickly incorporate amino acid from cognate tRNA into the peptide chain with a very low discard rate, greatly increasing the speed of cognate tRNA selection. At the same time, with proofreading, an acceptable level of accuracy is maintained. Given the error rate of transcription and the effect of error-rates on other cellular processes, there would be no point in being more accurate from the point of view of the viability or evolutionary fitness of the cell. This compromise between speed and accuracy in translation has long been known, but some of the underlying mechanisms have only recently become clear.

Base complementarity, which is at the source of the selection of the correct tRNA, is maintained stringently not because of the specificity of hydrogen bonding in a Watson-Crick base pair, but because all Watson-Crick base pairs are similar in shape and surface properties, especially at the minor groove. This isostericity of Watson-Crick base pairs was recognized at the very outset when the structure of the double helix was proposed, and it was recognized that A · T and G · C pairs had the same overall shape and would result in a helix of roughly uniform dimensions

regardless of sequence (206). Subsequently, it was recognized that minor grooves of nucleic acid had a shape that was largely invariant with sequence and, moreover, had hydrogen-bond acceptors at roughly the same position regardless of sequence (207). This offers a method of recognizing the geometry of correct pairing in a sequence-independent way. As it turns out, DNA and RNA polymerases as well as the ribosome all use this method to discriminate between correct and incorrect base pairing. Of these, the ribosome is undoubtedly the oldest, and the discrimination, which is done entirely using RNA, may date back to a primordial ribosome, which may have consisted almost entirely of RNA.

The observation that discrimination of base pairing can be done using RNA alone has evolutionary implications. On the basis of hydrogen bonding and base-stacking considerations, Watson-Crick base pairs are more favorable than other combinations. However, a self-replicating RNA molecule that relied only on this advantage would have been highly error prone, because of the small free-energy difference between correct and incorrect base pairs. Owing to its very high error rate, such a system would not have been able to evolve significantly in complexity. The structural work on the ribosome described here suggests that, even with RNA alone, it is possible to amplify the selection of Watson-Crick base pairs by recognition of their unique and characteristic shape. Thus an RNA molecule has within it both the ability to form base pairs and the ability to select them on the basis of geometry. Once an enzyme such as a primordial RNA polymerase had evolved to incorporate both of these features, the resulting higher fidelity of replication and gene expression would have allowed the evolution of much greater complexity. This critical shape recognition of Watson-Crick base pairs is now a general feature of enzymes involved in replication and gene expression, thus ensuring the ubiquity of base complementarity in life as we know it today.

ACKNOWLEDGMENTS

Work in the authors' laboratory was supported by the Medical Research Council (United Kingdom), the National Institutes of Health (United States) grant GM 67624, and the Agouron Institute. We thank Joachim Frank for kindly providing us the originals used in Figure 5.

The *Annual Review of Biochemistry* is online at http://biochem.annualreviews.org

LITERATURE CITED

1. Kunkel TA, Bebenek K. 2000. *Annu. Rev. Biochem.* 69:497–529
2. Rosenberger RF, Foskett G. 1981. *Mol. Gen. Genet.* 183:561–63
3. Rosenberger RF, Hilton J. 1983. *Mol. Gen. Genet.* 191:207–12
4. Kurland CG, Hughes D, Ehrenberg M. 1996. In *Escherichia coli and Salmonella typhimurium: Cellular and Molecular Biology*, ed. FC Neidhardt, R Curtiss III, JL Ingraham, ECC Lin, KB Low, B Magasanik, pp. 979–1004.

Washington, DC: Am. Soc. Microbiol. Press
5. Fersht AR. 1998. *Structure and Mechanism in Protein Science*. New York: Freeman
6. Fersht AR. 1977. *Biochemistry* 16: 1025–30
7. Nureki O, Vassylyev DG, Tateno M, Shimada A, Nakama T, et al. 1998. *Science* 280:578–82
8. Dock-Bregeon A, Sankaranarayanan R, Romby P, Caillet J, Springer M, et al. 2000. *Cell* 103:877–84
9. Fersht AR, Dingwall C. 1979. *Biochemistry* 18:2627–31
10. Freist W, Pardowitz I, Cramer F. 1985. *Biochemistry* 24:7014–23
11. Bouadloun F, Donner D, Kurland CG. 1983. *EMBO J.* 2:1351–56
12. Watson JD, Crick FHC. 1953. *Nature* 171:964–67
13. Crick FHC. 1957. *Symp. Biochem. Soc.* 14:25–26
14. Crick FHC, Griffith JS, Orgel LE. 1957. *Proc. Natl. Acad. Sci. USA* 43:416–21
15. Hoagland MB, Stephenson ML, Scott HF, Hecht LI, Zamecnik PC. 1958. *J. Biol. Chem.* 231:241–57
16. Holley RW, Apgar J, Everett GA, Madison JT, Marquisee M, et al. 1965. *Science* 147:1462–65
17. Pauling L. 1958. In *Arbeiten aus dem Gebiet der Naturstoffe* (*Festschr. Prof. Dr. Arthur Stoll Siebzigsten Geburtstag, 8 Jan. 1957*), pp. 597–602. Basel: Birkhäuser
18. Loftfield RB. 1963. *Biochem. J.* 89:82–92
19. Loftfield RB, Vanderjagt D. 1972. *Biochem. J.* 128:1353–56
20. Edelmann P, Gallant J. 1977. *Cell* 10: 131–37
21. Parker J, Flanagan J, Murphy J, Gallant J. 1981. *Mech. Ageing Dev.* 16:127–39
22. Davies J, Gilbert W, Gorini L. 1964. *Proc. Natl. Acad. Sci. USA* 51:883–90
23. Szer W, Ochoa S. 1964. *J. Mol. Biol.* 12:823–34
24. Weinstein IB, Friedman SM, Ochoa M Jr. 1966. *Cold Spring Harbor Symp. Quant. Biol.* 31:671–81
25. Jelenc PC, Kurland CG. 1979. *Proc. Natl. Acad. Sci. USA* 76:3174–78
26. Jaskunas SR, Cantor CR, Tinoco I Jr. 1968. *Biochemistry* 7:3164–78
27. Uhlenbeck OC, Baller J, Doty P. 1970. *Nature* 225:508–10
28. Eisinger J, Feuer B, Yamane T. 1970. *Proc. Natl. Acad. Sci. USA* 65:638–44
29. Eisinger J, Feuer B, Yamane T. 1971. *Nat. New Biol.* 231:126–28
30. Pongs O, Bald R, Reinwald E. 1973. *Eur. J. Biochem.* 32:117–25
31. Eisinger J. 1971. *Biochem. Biophys. Res. Commun.* 43:854–61
32. Grosjean H, Söll DG, Crothers DM. 1976. *J. Mol. Biol.* 103:499–519
33. Moras D, Dock AC, Dumas P, Westhof E, Romby P, et al. 1985. *J. Biomol. Struct. Dyn.* 3:479–93
34. Grosjean HJ, de Henau S, Crothers DM. 1978. *Proc. Natl. Acad. Sci. USA* 75:610–14
35. Thompson RC, Stone PJ. 1977. *Proc. Natl. Acad. Sci. USA* 74:198–202
36. Rodnina MV, Wintermeyer W. 2001. *Annu. Rev. Biochem.* 70:415–35
37. Xia T, SantaLucia J Jr, Burkard ME, Kierzek R, Schroeder SJ, et al. 1998. *Biochemistry* 37:14719–35
38. Kierzek R, Burkard ME, Turner DH. 1999. *Biochemistry* 38:14214–23
39. Mathews DH, Sabina J, Zuker M, Turner DH. 1999. *J. Mol. Biol.* 288:911–40
40. Freier SM, Sugimoto N, Sinclair A, Alkema D, Neilson T, et al. 1986. *Biochemistry* 25:3214–19
41. Fersht AR. 1987. *Trends Biochem. Sci.* 12:301–4
42. Pyle AM, Murphy FL, Cech TR. 1992. *Nature* 358:123–28
43. Pyle AM, Cech TR. 1991. *Nature* 350: 628–31

44. Pyle AM, McSwiggen JA, Cech TR. 1990. *Proc. Natl. Acad. Sci. USA* 87: 8187–91
45. Bevilacqua PC, Turner DH. 1991. *Biochemistry* 30:10632–40
46. SantaLucia J Jr, Kierzek R, Turner DH. 1992. *Science* 256:217–19
47. Freier SM, Kierzek R, Caruthers MH, Neilson T, Turner DH. 1986. *Biochemistry* 25:3209–13
48. Sugimoto N, Kierzek R, Turner DH. 1987. *Biochemistry* 26:4559–62
49. Sugimoto N, Kierzek R, Freier SM, Turner DH. 1986. *Biochemistry* 25: 5755–59
50. Lipsett MN, Heppel LA, Bradley DF. 1960. *Biochim. Biophys. Acta* 41:175–77
51. Lipsett MN, Heppel LA, Bradley DF. 1961. *J. Biol. Chem.* 236:857–63
52. Lipsett MN. 1964. *J. Biol. Chem.* 239: 1256–60
53. McLaughlin CS, Dondon J, Grunberg-Manago M, Michelson AM, Saunders G. 1966. *Cold Spring Harbor Symp. Quant. Biol.* 31:601–10
54. Crick FHC. 1963. *Prog. Nucleic Acid Res. Mol. Biol.* 1:164–217
55. Gorini L, Kataja E. 1964. *Proc. Natl. Acad. Sci. USA* 51:487–93
56. Gorini L, Jacoby GA, Breckenridge L. 1966. *Cold Spring Harbor Symp. Quant. Biol.* 31:657–64
57. Gorini L. 1974. In *Ribosomes*, ed. M Nomura, A Tissiéres, P Lengyel, pp. 791–803. Cold Spring Harbor, NY: Cold Spring Harbor Lab.
58. Ozaki M, Mizushima S, Nomura M. 1969. *Nature* 222:333–39
59. Chakrabarti S, Gorini L. 1975. *J. Bacteriol.* 121:670–74
60. Kurland CG, Ehrenberg M. 1984. *Prog. Nucleic Acid Res. Mol. Biol.* 31:191–219
61. Gorini L, Rosset R, Zimmermann RA. 1967. *Science* 157:1314–17
62. Brownstein BL, Lewandowski LJ. 1967. *J. Mol. Biol.* 25:99–109
63. Rosset R, Gorini L. 1969. *J. Mol. Biol.* 39:95–112
64. Bjare U, Gorini L. 1971. *J. Mol. Biol.* 57:423–35
65. Zimmermann RA, Garvin RT, Gorini L. 1971. *Proc. Natl. Acad. Sci. USA* 68:2263–67
66. Hasenbank R, Guthrie C, Stoffler G, Wittmann HG, Rosen L, Apirion D. 1973. *Mol. Gen. Genet.* 127:1–18
67. Piepersberg W, Bock A, Wittmann HG. 1975. *Mol. Gen. Genet.* 140:91–100
68. Biswas DK, Gorini L. 1972. *J. Mol. Biol.* 64:119–34
69. Hirsh D. 1971. *J. Mol. Biol.* 58:439–58
70. Hirsh D, Gold L. 1971. *J. Mol. Biol.* 58:459–68
71. Buckingham RH, Kurland CG. 1977. *Proc. Natl. Acad. Sci. USA* 74:5496–98
72. Gorini L. 1971. *Nat. New Biol.* 234:261–64
73. Kirsebom LA, Isaksson LA. 1985. *Proc. Natl. Acad. Sci. USA* 82:717–21
74. Kirsebom LA, Amons R, Isaksson LA. 1986. *Eur. J. Biochem.* 156:669–75
75. Eigen M, de Maeyer L. 1966. *Naturwissenschaften* 53:50–57
76. Potapov AP. 1982. *FEBS Lett.* 146:5–8
77. Ninio J. 1974. *J. Mol. Biol.* 84:297–313
78. Hopfield JJ. 1974. *Proc. Natl. Acad. Sci. USA* 71:4135–39
79. Ninio J. 1975. *Biochimie* 57:587–95
80. Blomberg C, Ehrenberg M, Kurland CG. 1980. *Q. Rev. Biophys.* 13:231–54
81. Ruusala T, Ehrenberg M, Kurland CG. 1982. *EMBO J.* 1:741–45
82. Thompson RC, Dix DB, Gerson RB, Karim AM. 1981. *J. Biol. Chem.* 256:6676–81
83. Ruusala T, Kurland CG. 1984. *Mol. Gen. Genet.* 198:100–4
84. Thompson RC. 1988. *Trends Biochem. Sci.* 13:91–93
85. Thompson RC, Karim AM. 1982. *Proc. Natl. Acad. Sci. USA* 79:4922–26
86. Czworkowski J, Moore PB. 1996. *Prog. Nucleic Acid Res. Mol. Biol.* 54:293–332

87. Hausner TP, Geigenmuller U, Nierhaus KH. 1988. *J. Biol. Chem.* 263:13103–11
88. Geigenmuller U, Nierhaus KH. 1990. *EMBO J.* 9:4527–33
89. Rodnina MV, Fricke R, Wintermeyer W. 1994. *Biochemistry* 33:12267–75
90. Rodnina MV, Fricke R, Kuhn L, Wintermeyer W. 1995. *EMBO J.* 14:2613–19
91. Pape T, Wintermeyer W, Rodnina MV. 1998. *EMBO J.* 17:7490–97
92. Pape T, Wintermeyer W, Rodnina MV. 1999. *EMBO J.* 18:3800–7
93. Vorstenbosch E, Pape T, Rodnina MV, Kraal B, Wintermeyer W. 1996. *EMBO J.* 15:6766–74
94. Kjeldgaard M, Nyborg J. 1992. *J. Mol. Biol.* 223:721–42
95. Berchtold H, Reshetnikova L, Reiser CO, Schirmer NK, Sprinzl M, Hilgenfeld R. 1993. *Nature* 365:126–32
96. Kjeldgaard M, Nissen P, Thirup S, Nyborg J. 1993. *Structure* 1:35–50
97. Gromadski KB, Rodnina MV. 2004. *Mol. Cell* 13:191–200
98. Noller HF, Chaires JB. 1972. *Proc. Natl. Acad. Sci. USA* 69:3115–18
99. Moazed D, Noller HF. 1990. *J. Mol. Biol.* 211:135–45
100. Powers T, Noller HF. 1990. *Proc. Natl. Acad. Sci. USA* 87:1042–46
101. Yoshizawa S, Fourmy D, Puglisi JD. 1999. *Science* 285:1722–25
102. Moazed D, Noller HF. 1987. *Nature* 327:389–94
103. Purohit P, Stern S. 1994. *Nature* 370: 659–62
104. Fourmy D, Recht MI, Blanchard SC, Puglisi JD. 1996. *Science* 274:1367–71
105. Fourmy D, Yoshizawa S, Puglisi JD. 1998. *J. Mol. Biol.* 277:333–45
106. van Loock MS, Easterwood TR, Harvey SC. 1999. *J. Mol. Biol.* 285:2069–78
107. Pape T, Wintermeyer W, Rodnina MV. 2000. *Nat. Struct. Biol.* 7:104–7
108. Yonath A, Mussig J, Tesche B, Lorenz S, Erdmann VA, Wittmann HG. 1980. *Biochem. Int.* 1:428–35
109. Trakhanov SD, Yusupov MM, Agalarov SC, Garber MB, Ryazantsev SN, et al. 1987. *FEBS Lett.* 220:319–22
110. Glotz C, Müssig J, Gewitz HS, Makowski I, Arad T, et al. 1987. *Biochem. Int.* 15:953–60
111. Yonath A, Glotz C, Gewitz HS, Bartels KS, von Böhlen K, et al. 1988. *J. Mol. Biol.* 203:831–34
112. von Böhlen K, Makowski I, Hansen HAS, Bartels H, Berkovitch-Yellin Z, et al. 1991. *J. Mol. Biol.* 222:11–15
113. Yonath A, Harms J, Hansen HA, Bashan A, Schlunzen F, et al. 1998. *Acta Crystallogr. A* 54:945–55
114. Clemons WM J Jr, May JL, Wimberly BT, McCutcheon JP, Capel MS, Ramakrishnan V. 1999. *Nature* 400:833–40
115. Cate JH, Yusupov MM, Yusupova GZ, Earnest TN, Noller HF. 1999. *Science* 285:2095–104
116. Ban N, Freeborn B, Nissen P, Penczek P, Grassucci RA, et al. 1998. *Cell* 93:1105–15
117. Ban N, Nissen P, Hansen J, Capel M, Moore PB, Steitz TA. 1999. *Nature* 400:841–47
118. Wimberly BT, Brodersen DE, Clemons WM Jr, Morgan-Warren RJ, Carter AP, et al. 2000. *Nature* 407:327–39
119. Ban N, Nissen P, Hansen J, Moore PB, Steitz TA. 2000. *Science* 289:905–20
120. Schluenzen F, Tocilj A, Zarivach R, Harms J, Gluehmann M, et al. 2000. *Cell* 102:615–23
121. Brodersen DE, Clemons WM Jr, Carter AP, Wimberly BT, Ramakrishnan V. 2002. *J. Mol. Biol.* 316:725–68
122. Pioletti M, Schlunzen F, Harms J, Zarivach R, Gluhmann M, et al. 2001. *EMBO J.* 20:1829–39
123. Yusupov MM, Yusupova GZ, Baucom A, Lieberman K, Earnest TN, et al. 2001. *Science* 292:883–96
124. Carter AP, Clemons WM Jr, Brodersen DE, Morgan-Warren RJ, Wimberly BT, Ramakrishnan V. 2000. *Nature* 407:340–48

125. Vicens Q, Westhof E. 2001. *Structure* 9:647–58
126. Lynch SR, Gonzalez RL, Puglisi JD. 2003. *Structure* 11:43–53
127. Carter AP, Clemons WM Jr, Brodersen DE, Morgan-Warren RJ, Hartsch T, et al. 2001. *Science* 291:498–501
128. Ogle JM, Brodersen DE, Clemons WM Jr, Tarry MJ, Carter AP, Ramakrishnan V. 2001. *Science* 292:897–902
129. Doherty EA, Batey RT, Masquida B, Doudna JA. 2001. *Nat. Struct. Biol.* 8: 339–43
130. Nissen P, Ippolito JA, Ban N, Moore PB, Steitz TA. 2001. *Proc. Natl. Acad. Sci. USA* 98:4899–903
131. Battle DJ, Doudna JA. 2002. *Proc. Natl. Acad. Sci. USA* 99:11676–81
132. Ogle JM, Murphy FV, Tarry MJ, Ramakrishnan V. 2002. *Cell* 111:721–32
133. Tronrud DE, Holden HM, Matthews BW. 1987. *Science* 235:571–74
134. Bartlett PA, Marlowe CK. 1987. *Science* 235:569–71
135. van Heel M, Gowen B, Matadeen R, Orlova EV, Finn R, et al. 2000. *Q. Rev. Biophys.* 33:307–69
136. Frank J. 2002. *Annu. Rev. Biophys. Biomol. Struct.* 31:303–19
137. Douglass J, Blumenthal T. 1979. *J. Biol. Chem.* 254:5383–87
138. Vogeley L, Palm GJ, Mesters JR, Hilgenfeld R. 2001. *J. Biol. Chem.* 276:17149–55
139. Simonson AB, Lake JA. 2002. *Nature* 416:281–85
140. Stark H, Rodnina MV, Rinke-Appel J, Brimacombe R, Wintermeyer W, van Heel M. 1997. *Nature* 389:403–6
141. Moazed D, Noller HF. 1989. *Nature* 342:142–48
142. Powers T, Noller HF. 1994. *J. Mol. Biol.* 235:156–72
143. Valle M, Sengupta J, Swami NK, Grassucci RA, Burkhardt N, et al. 2002. *EMBO J.* 21:3557–67
144. Stark H, Rodnina MV, Wieden HJ, Zemlin F, Wintermeyer W, van Heel M. 2002. *Nat. Struct. Biol.* 9:849–54
145. Nissen P, Kjeldgaard M, Thirup S, Polekhina G, Reshetnikova L, et al. 1995. *Science* 270:1464–72
146. Valle M, Zavialov A, Li W, Stagg SM, Sengupta J, et al. 2003. *Nat. Struct. Biol.* 10:899–906
147. Ogle JM, Carter AP, Ramakrishnan V. 2003. *Trends Biochem. Sci.* 28:259–66
148. Rodnina MV, Pape T, Fricke R, Kuhn L, Wintermeyer W. 1996. *J. Biol. Chem.* 271:646–52
149. Vila-Sanjurjo A, Ridgeway WK, Seymaner V, Zhang W, Santoso S, et al. 2003. *Proc. Natl. Acad. Sci. USA* 100: 8682–87
150. Gavrilova LP, Kostiashkina OE, Koteliansky VE, Rutkevitch NM, Spirin AS. 1976. *J. Mol. Biol.* 101:537–52
151. Woese C. 1970. *Nature* 226:817–20
152. Stagg SM, Valle M, Agrawal RK, Frank J, Harvey SC. 2002. *RNA* 8:1093–94
153. Yates JL. 1979. *J. Biol. Chem.* 254: 11550–54
154. Bilgin N, Claesens F, Pahverk H, Ehrenberg M. 1992. *J. Mol. Biol.* 224:1011–27
155. Rodnina MV, Daviter T, Gromadski K, Wintermeyer W. 2002. *Biochimie* 84: 745–54
156. Gromadski KB, Rodnina MV. 2004. *Nat. Struct. Mol. Biol.* 11:316–22
157. Kurland CG, Rigler R, Ehrenberg M, Blomberg C. 1975. *Proc. Natl. Acad. Sci. USA* 72:4248–51
158. Yarus M, Smith D. 1995. In *tRNA: Structure, Biosynthesis and Function*, ed. D Söll, U RajBhandary, pp. 443–68. Washington, DC: Am. Soc. Microbiol. Press
159. Favre A, Buckingham R, Thomas G. 1975. *Nucleic Acids Res.* 2:1421–31
160. Vacher J, Buckingham RH. 1979. *J. Mol. Biol.* 129:287–94
161. Smith D, Yarus M. 1989. *J. Mol. Biol.* 206:489–501
162. Smith D, Yarus M. 1989. *J. Mol. Biol.* 206:503–11

163. Schultz DW, Yarus M. 1994. *J. Mol. Biol.* 235:1395–405
164. Schultz DW, Yarus M. 1994. *J. Mol. Biol.* 235:1381–94
165. Yarus M, Valle M, Frank J. 2003. *RNA* 9:384–85
166. Piepenburg O, Pape T, Pleiss JA, Wintermeyer W, Uhlenbeck OC, Rodnina MV. 2000. *Biochemistry* 39:1734–38
167. Robertus JD, Ladner JE, Finch JT, Rhodes D, Brown RS, et al. 1974. *Nature* 250:546–51
168. Hilgenfeld R, Mesters J, Hogg T. 2000. In *The Ribosome: Structure, Function, Antibiotics and Cellular Interactions*, ed. RA Garrett, SR Douthwaite, A Liljas, AT Matheson, PB Moore, HF Noller, pp. 347–57. Washington, DC: Am. Soc. Microbiol. Press
169. Krab IM, Parmeggiani A. 2002. *Prog. Nucleic Acid Res. Mol. Biol.* 71:513–51
170. Alexander C, Bilgin N, Lindschau C, Mesters JR, Kraal B, et al. 1995. *J. Biol. Chem.* 270:14541–47
171. Tapprich WE, Dahlberg AE. 1990. *EMBO J.* 9:2649–55
172. Bilgin N, Ehrenberg M. 1994. *J. Mol. Biol.* 235:813–24
173. Tapio S, Isaksson LA. 1991. *Eur. J. Biochem.* 202:981–84
174. Kothe U, Wieden HJ, Mohr D, Rodnina MV. 2004. *J. Mol. Biol.* 336:1011–21
175. McCarthy BJ, Holland JJ. 1965. *Proc. Natl. Acad. Sci. USA* 54:880–86
176. Potapov AP, Triana-Alonso FJ, Nierhaus KH. 1995. *J. Biol. Chem.* 270:17680–84
177. Brodersen DE, Clemons WM Jr, Carter AP, Morgan-Warren RJ, Wimberly BT, Ramakrishnan V. 2000. *Cell* 103:1143–54
178. Rheinberger HJ, Nierhaus KH. 1986. *J. Biol. Chem.* 261:9133–39
179. Lodmell JS, Dahlberg AE. 1997. *Science* 277:1262–67
180. Lodmell JS, Gutell RR, Dahlberg AE. 1995. *Proc. Natl. Acad. Sci. USA* 92: 10555–59
181. Velichutina IV, Dresios J, Hong JY, Li C, Mankin A, et al. 2000. *RNA* 6:1174–84
182. Carter AP. 2002. *Structural studies of the 30S ribosomal subunit*. PhD thesis. Univ. Cambridge, Cambridge, UK
183. Rodriguez-Correa D, Dahlberg AE. 2004. *RNA* 10:28–33
184. Sprinzl M, Horn C, Brown M, Ioudovitch A, Steinberg S. 1998. *Nucleic Acids Res.* 26:148–53
185. Agris PF. 2004. *Nucleic Acids Res.* 32:223–38
186. Yarian C, Marszalek M, Sochacka E, Malkiewicz A, Guenther R, et al. 2000. *Biochemistry* 39:13390–95
187. Yarian C, Townsend H, Czestkowski W, Sochacka E, Malkiewicz AJ, et al. 2002. *J. Biol. Chem.* 277:16391–95
188. Konevega AL, Soboleva NG, Makhno VI, Semenkov YP, Wintermeyer W, et al. 2004. *RNA* 10:90–101
188a. Murphy FV, Ramakrishnan V, Malkiewicz A, Agris PF. 2004. *Nat. Struct. Mol. Biol.* 11:1186–91
189. Atkins JF, Elseviers D, Gorini L. 1972. *Proc. Natl. Acad. Sci. USA* 69:1192–95
190. Riddle DL, Carbon J. 1973. *Nat. New Biol.* 242:230–34
191. Roth JR. 1981. *Cell* 24:601–2
192. Stahl G, McCarty GP, Farabaugh PJ. 2002. *Trends Biochem. Sci.* 27:178–83
193. Hansen TM, Baranov PV, Ivanov IP, Gesteland RF, Atkins JF. 2003. *EMBO Rep.* 4:499–504
194. Marquez V, Wilson DN, Tate WP, Triana-Alonso F, Nierhaus KH. 2004. *Cell* 118:45–55
195. Doublie S, Tabor S, Long AM, Richardson CC, Ellenberger T. 1998. *Nature* 391:251–58
196. Cheetham GM, Steitz TA. 1999. *Science* 286:2305–9
197. Johnson SJ, Beese LS. 2004. *Cell* 116:803–16
198. Ling H, Boudsocq F, Woodgate R, Yang W. 2001. *Cell* 107:91–102

199. Morales JC, Kool ET. 1998. *Nat. Struct. Biol.* 5:950–54
200. Kool ET. 2002. *Annu. Rev. Biochem.* 71: 191–219
201. Steitz TA. 1999. *J. Biol. Chem.* 274: 17395–98
202. Doublie S, Sawaya MR, Ellenberger T. 1999. *Struct. Fold Des.* 7:R31–35
203. Beard WA, Wilson SH. 2003. *Structure* 11:489–96
203a. Blanchard SC, Gonzalez RL, Kim HD, Chu S, Puglisi JD. 2004. *Nat. Struct. Mol. Biol.* 11:1008–14
204. Sanbonmatsu KY, Joseph S. 2003. *J. Mol. Biol.* 328:33–47
205. LaRiviere FJ, Wolfson AD, Uhlenbeck OC. 2001. *Science* 294:165–68
206. Watson JD, Crick FHC. 1953. *Nature* 171:737–38
207. Seeman NC, Rosenberg JM, Rich A. 1976. *Proc. Natl. Acad. Sci. USA* 73: 804–8
208. Nissen P, Kjeldgaard M, Thirup S, Clark BF, Nyborg J. 1996. *Biochimie* 78:921–33

Annual Review of Biochemistry
Volume 74, 2005

CONTENTS